Journal of Paleontology, 97(1), 2023, p. 1–25

0022-3360/23/1937-2337
doi: 10.1017/jpa.2022.82

JOURNAL OF PALEONTOLOGY
A PUBLICATION OF THE Paleontological SOCIETY

Progress in understanding middle Eocene nassellarian (Radiolaria, Polycystinea) diversity; new insights from the western equatorial Atlantic Ocean

Mathias Meunier* and Taniel Danelian

Univ. Lille, CNRS, UMR 8198-Evo-Eco-Paleo, F-59000 Lille, France <mathias.meunier@univ-lille.fr>, <taniel.danelian@univ-lille.fr>

Abstract.—Middle Eocene deep-sea sediment sequences cored at Ocean Drilling Program Site 1260 (Leg 207; equatorial Atlantic Ocean) yielded diverse and abundant radiolarian faunas that are conducive to biostratigraphic and palaeoceanographic research, as well as to the study of radiolarian diversity dynamics during this epoch of significant climate changes. However, many species present in these sediments still have not been formally described and are therefore neglected in most biodiversity surveys. In an effort to improve the taxonomic resolution of middle Eocene radiolarians, 15 new species of nassellarians are described and illustrated. The species are: *Cymaetron*? *dilatatus* n. sp., *Eucyrtidium levisaltatrix* n. sp. (Eucyrtidiidae), *Siphocampe pollen* n. sp., *Spirocyrtis*? *renaudiei* n. sp. (Artostrobiidae), *Pterocyrtidium eep* n. sp. (Rhopalosyringiidae), *Petalospyris cometa* n. sp., *Petalospyris castanea* n. sp. (Cephalospyrididae), *Velicucullus armatus* n. sp. (Theophormididae), *Lychnocanium nimrodi* n. sp. (Lithochytrididae), *Aphetocyrtis zamenhofi* n. sp., *Aphetocyrtis*? *columboi* n. sp., *Aphetocyrtis*? *spheniscus* n. sp. (Lophocyrtiidae), *Albatrossidium regis* n. sp., *Albatrossidium annikasanfilippoae* n. sp., and *Phormocyrtis lazari* n. sp. (Pterocorythidae). Stratigraphic range data are provided for each new species, as well as the orbitally tuned ages for their first and last occurrences. In addition to these new species, we also illustrate and document the stratigraphic distribution of four species described in early radiolarian studies and rarely reported since.

UUID: http://zoobank.org/b5993e6b-659b-4220-80c2-c6ddccc13793

Introduction

Reconstructing paleodiversity dynamics of Eocene tropical radiolarians is primarily hampered by our incomplete taxonomic knowledge of these organisms. Indeed, despite being studied for nearly two centuries (Ehrenberg, 1839), we are still far from having fully documented and described all of the species preserved in the Eocene fossil record. The first major contribution to the taxonomy of Eocene radiolarians is attributed to Ehrenberg (1874), who described 265 new species from middle Eocene to lower Oligocene pelagic sequences that crop out today on the Barbados Island (Saunders et al., 1984; Ogane et al., 2009), 85 of which were subsequently illustrated in Ehrenberg (1876). In his famous monograph, Haeckel (1887) also introduced ~200 middle Eocene radiolarian species from Barbados onshore samples, including illustrations for only half of them. In addition to this body of taxonomic work, several authors sporadically published new species and genera throughout the late nineteenth century (Bury, 1862; Bütschli, 1882a, b; Carter, 1893, 1895, 1896a, b, c, d, e; Sutton, 1896a, b, c, d). However, numerous species described in these early radiolarian studies have not been reported since, and there are still many uncertainties about their stratigraphic range, their biogeographic distribution, and the precise extent of their intraspecific variation (Ogane et al., 2009).

Although little taxonomic progress was achieved on tropical Eocene radiolarians during the first half of the twentieth century (e.g., Brandt, 1935), two important publications by Clark and Campbell (1942, 1945) that marked this period were devoted to the study of middle–late Eocene radiolarian faunas from three Californian shale formations, and resulted in the description of 157 new species (Blueford, 1988). The subsequent advent of scientific ocean drilling during the 1960s and 1970s marked a turning point in the history of Cenozoic radiolarian taxonomy. The increase of deep-sea sediment recovery allowed extensive studies of radiolarian assemblages across the world, and renewed interest in describing radiolarian diversity (e.g., Riedel and Sanfilippo, 1970, 1971, 1978; Petrushevskaya and Kozlova, 1972; Foreman, 1973; Sanfilippo and Riedel, 1973). The primary goal of these studies was biostratigraphy, and thus they were usually focused on a limited number of stratigraphically useful species that are often abundant in the Eocene fossil record. As a consequence, many rare morphotypes of no biostratigraphic value, or those belonging to morphologically complex taxa, remained undescribed and were neglected in most taxonomic surveys. Concurrently with this biostratigraphic work, some nassellarian families have also been the subjects of more detailed and exhaustive taxonomic investigations, leading to the establishment of several evolutionary lineages (e.g., Nigrini, 1977; Sanfilippo and Riedel, 1982, 1992; Sanfilippo and Caulet, 1998).

*Corresponding author

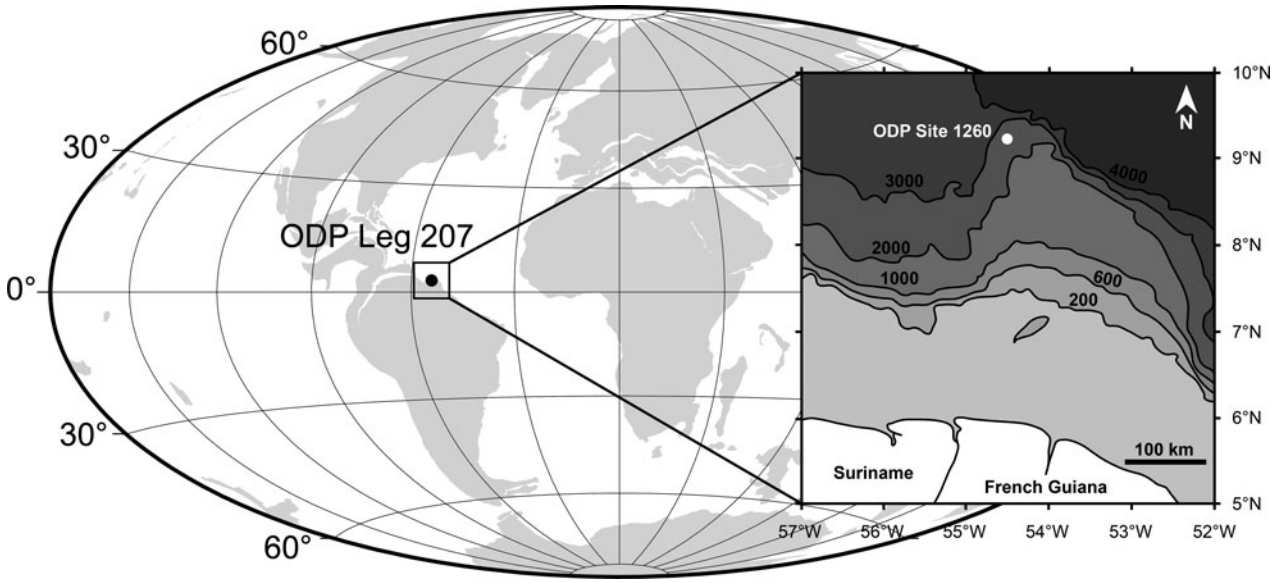

Figure 1. Middle Eocene (ca. 40 Ma) paleogeographic map showing the location of Demerara Rise (ODP Leg 207) in the western equatorial Atlantic Ocean. The square shows the detailed location of ODP Site 1260 on a modern bathymetric map (modified after Wang et al., 2016). Paleogeographic reconstruction drawn after ODSN Plate Tectonic Reconstruction Service (http://www.odsn.de/odsn/services/paleomap/paleomap.html).

In an effort to improve the taxonomic resolution of tropical Eocene radiolarians, 15 new nassellarian species belonging to 11 genera and seven families are described and illustrated from the upper middle Eocene sequences drilled at Ocean Drilling Program Site 1260 (Leg 207; western Atlantic Ocean). Among the undescribed morphotypes encountered in this material, we chose to describe the most abundant and morphologically distinct, to best circumscribe the morphological diversity of each new species. As a consequence, some potentially new species only represented by one or a few isolated specimens were excluded from this analysis. Information is also provided for the stratigraphic range of each new species, as well as the orbitally tuned ages for the first and last occurrences of most of them. Relationships to previously described species are also suggested. Finally, three species described in early radiolarian studies and rarely reported since are illustrated and discussed.

Materials and methods

Materials.—All samples investigated in this study came from ODP Leg 207, Site 1260 (9°16′N, 54°32′W) located on the northwestern slope of Demerara Rise, a continental shelf off Surinam and French Guiana (Fig. 1). The site is situated between 9°N and 10°N latitude today, but according to paleomagnetic data, its position during the middle Eocene is estimated at paleolatitude ~1°N (Suganuma and Ogg, 2006). Two holes (1260A and 1260B) recovered Paleogene sediments at a water depth of 2549 meters below sea floor (mbsf), enabling the study of an expanded and almost continuous sedimentary sequence extending from the lower Albian to the middle Eocene (Shipboard Scientific Party, 2004). The middle Eocene interval of ODP Site 1260 is composed of greenish white foraminifer-nannofossil chalk with abundant, well-preserved radiolarians and diatoms (Shipboard Scientific Party, 2004; Danelian et al., 2005, 2007; Renaudie et al., 2010). In this study, we focused on the richest radiolarian interval; a 91.72 m thick sequence ranging from 43.77–39.83 Ma that corresponds to the late middle Eocene (middle Lutetian to middle Bartonian). Fifty-five samples were selected from 10 cores (15R to 6R) from Hole 1260A, resulting in an average inter-sample spacing of ~1.67 m and a mean age resolution of ca. 71,600 years.

A well-defined cyclostratigraphic framework was developed for ODP Site 1260 using X-ray fluorescence core scanning (Westerhold and Röhl, 2013). Astrochronological calibration, which is available throughout the sequence every 2 cm of sediment, allowed each sample to be dated with a high accuracy. Whenever there was absence of calibration for parts of Hole 1260A, the absolute ages of these samples were estimated based on the tuned ages provided for samples at the same depth located in Hole 1260B.

Methods.—Samples were processed following the protocol outlined in Sanfilippo et al. (1985). First, 1–2 cm^2 of untreated sediments were placed in a beaker and soaked in ~10% hydrogen peroxide (H_2O_2) and ~30% hydrochloric acid (HCl) to remove organic matter and carbonate fraction, respectively. The resulting residues were subsequently washed through a 45 μm sieve to eliminate clay, small diatom frustules, and radiolarian fragments. We chose this relatively fine mesh to improve the recovery of smaller radiolarian species that may be lost by the use of larger mesh. Then, 1–4 slides were prepared for each sample by using a few mg of cleaned residues, evenly scattered on a coverslip according to the preparation method described by Witkowski et al. (2012). When dry, the coverslips were mounted on standard glass slides using Norland Optical Adhesive 61 (refractive index 1.56).

All slides were examined systematically for radiolarians using a Zeiss Axio Imager.A2 as a transmitted light microscope, fitted with a Zeiss AxioCam ERc5s digital camera. For each

https://doi.org/10.1017/jpa.2022.82 Published online by Cambridge University Press

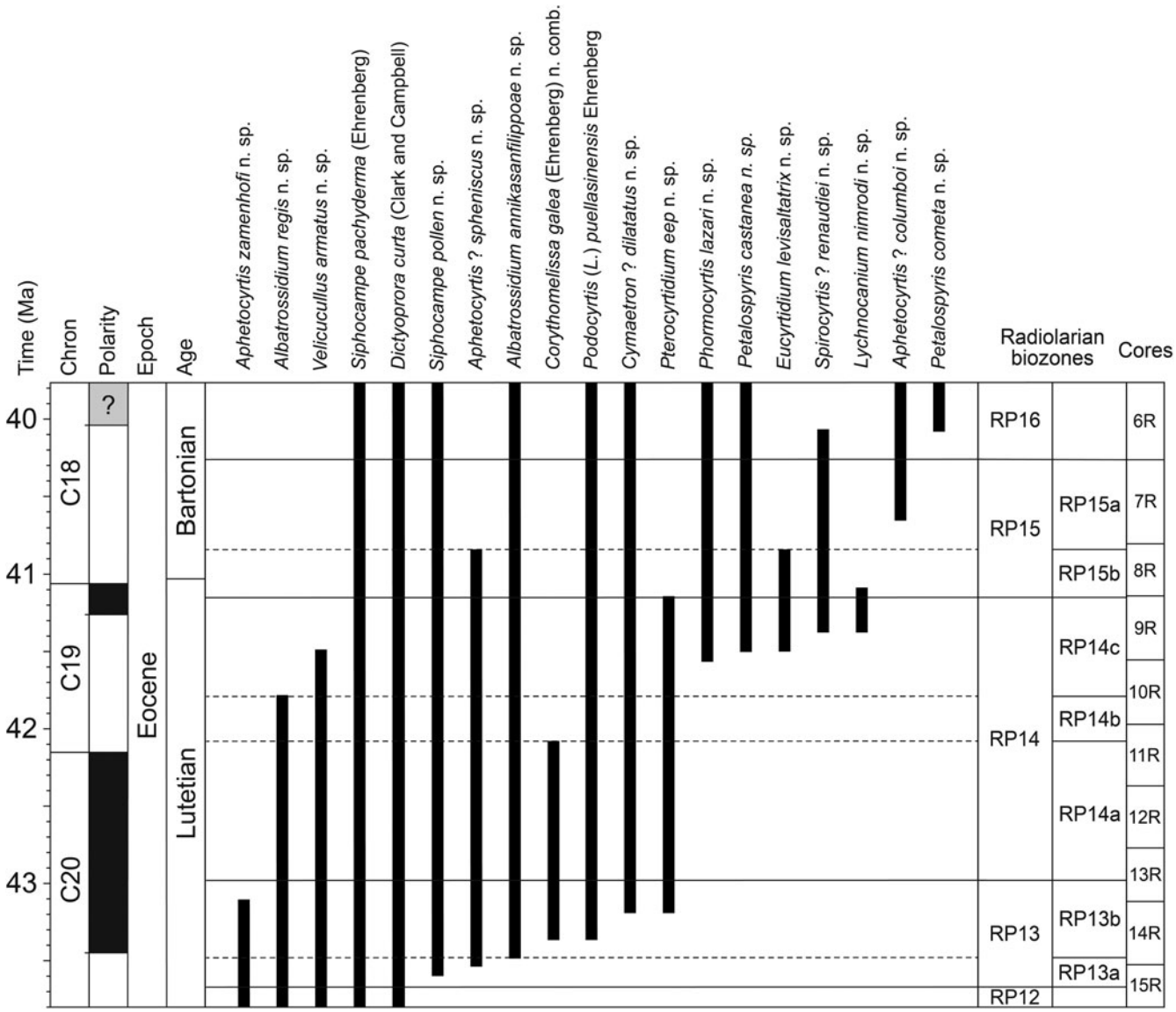

Figure 2. Range chart of 19 selected radiolarian species from the middle Eocene of ODP Site 1260 (Demerara Rise, western equatorial Atlantic). Geomagnetic timescale after calibration of Suganuma and Ogg (2006); radiolarian biozonations after Meunier and Danelian (2022).

illustrated specimen, a series of 5–10 pictures captured at different focal distances were z-stacked using Helicon Focus v.7.6.6 (HeliconSoft) to create a composite picture entirely in focus.

In the following section, dimensions are based on a maximum number of specimens observed at different depths in the sedimentary sequence, in order to represent the intraspecific variation throughout the stratigraphic range of the species. Measurements were directly made on specimen pictures using the image processing and analysis software ImageJ (Schneider et al., 2012).

The radiolarian biozonation applied herein is the one introduced by Riedel and Sanfilippo (1970, 1971, 1978) and Sanfilippo et al. (1985), and recently refined by Meunier and Danelian (2022), with the introduction of some subzones. Stratigraphic occurrences of species are shown in Figure 2 (see also Supplement Data 1 for the occurrence of each studied species per sample) and related bioevents are summarized in Table 1, with their tuned age at ODP Site 1260.

Repository and institutional abbreviation.—All holotypes and figured specimens (Figs. 3–7) are housed at the public paleontological collection of the University of Lille (USTL), France. Specimens are located according to hole number, core number, section number, interval depth, and England finder coordinates.

Systematic paleontology

The higher level classification adopted for this study is based on the most recent and comprehensive radiolarian classification provided by Suzuki et al. (2021). In the case of species already described, we used combinations derived from O'Dogherty et al. (2021).

The terminology used to designate different parts of the fundamental nassellarian spicule is based on Petrushevskaya (1984). Features specific to the family Cephalospyrididae follow Goll (1968, p. 1413, text-figure 6) and features specific to the

https://doi.org/10.1017/jpa.2022.82 Published online by Cambridge University Press

Table 1. Summary of first occurrences (FO) and last occurrences (LO) at ODP Site 1260, drilled on Demerara Rise in the western equatorial Atlantic. The estimated tuned age and revised meters composite depth (rmcd) are after Westerhold and Röhl (2013).

ODP Site 1260		Depth (rmcd)	Tuned age (Ma)	
Radiolarian bioevents	Core, section, interval (cm) Base/top	Base/top	Base/top	Midpoint
FO *Petalospyris cometa* n. sp.	6R-5W, 55–57/6R-4W, 55–57	44.75/43.25	40.11/40.04	40.08
LO *Spirocyrtis*? *renaudiei* n. sp.	6R-5W, 55–57/6R-4W, 55–57	44.75/43.25	40.11/40.04	40.08
FO *Aphetocyrtis*? *columboi* n. sp.	7R-6W, 54–56/7R-4W, 54–56	56.04/53.04	40.73/40.57	40.65
LO *Eucyrtidium levisaltatrix* n. sp.	7R-6W, 54–56/7R-4W, 54–56	56.04/53.04	40.73/40.57	40.65
LO *Aphetocyrtis*? *spheniscus* n. sp.	8R-3W, 54–56/7R-6W, 54–56	61.24/56.04	40.96/40.73	40.85
LO *Lychnocanium nimrodi* n. sp.	8R-6W, 54–56/8R-5W, 54–56	65.74/64.24	41.12/41.07	41.10
LO *Pterocyrtidium eep* n. sp.	9R-1W, 55–57/8R-6W, 54–56	66.85/65.74	41.18/41.12	41.15
FO *Lychnocanium nimrodi* n. sp.	9R-5W, 55–57/9R-4W, 55–57	72.85/71.35	41.40/41.34	41.37
FO *Spirocyrtis*? *renaudiei* n. sp.	9R-5W, 55–57/9R-4W, 55–57	72.85/71.35	41.40/41.34	41.37
FO *Eucyrtidium levisaltatrix* n. sp.	9R-7W, 55–57/9R-6W, 55–57	75.85/74.35	41.53/41.46	41.50
FO *Petalospyris castanea* n. sp.	9R-7W, 55–57/9R-6W, 55–57	75.85/74.35	41.53/41.46	41.50
LO *Velicucullus armatus* n. sp.	9R-7W, 55–57/9R-6W, 55–57	75.85/74.35	41.53/41.46	41.50
FO *Phormocyrtis lazari* n. sp.	10R-1W, 55–57/9R-7W, 55–57	77.33/75.85	41.59/41.53	41.56
LO *Albatrossidium regis* n. sp.	10R-5W, 55–57/10R-3W, 55–57	83.33/80.33	41.85/41.73	41.79
LO *Corythomelissa galea* (Ehrenberg) n. comb.	11R-3W, 55–57/11R-2W, 55–57	89.55/88.05	42.12/42.05	42.09
LO *Aphetocyrtis zamenhofi* n. sp.	14R-1W, 55–57/13R-6W, 54–56	116.02/112.74	43.16/43.06	43.11
FO *Cymaetron*? *dilatatus* n. sp.	14R-2W, 55–57/14R-1W, 55–57	117.52/116.02	43.21/43.16	43.19
FO *Pterocyrtidium eep* n. sp.	14R-2W, 55–57/14R-1W, 55–57	117.52/116.02	43.21/43.16	43.19
FO *Corythomelissa galea* (Ehrenberg) n. comb.	14R-5W, 55–57/14R-4W, 55–57	122.02/120.52	43.39/43.33	43.36
FO *Podocyrtis* (*L.*) *puellasinensis* Ehrenberg	14R-5W, 55–57/14R-4W, 55–57	122.02/120.52	43.39/43.33	43.36
FO *Albatrossidium annikasanfilippoae* n. sp.	14R-7W, 55–57/14R-6W, 55–57	125.02/123.52	43.51/43.45	43.48
FO *Aphetocyrtis*? *spheniscus* n. sp.	15R-1W, 55–57/14R-7W, 55–57	125.97/125.02	43.55/43.51	43.53
FO *Siphocampe pollen* n. sp.	15R-2W, 55–57/15R-1W, 55–57	127.47/125.97	43.63/43.55	43.59

family Lophocyrtiidae follow Sanfilippo and Caulet (1998, p. 6, text-figure 2).

Infrakingdom Rhizaria Cavalier-Smith, 2002, emend. Cavalier-Smith (2003)
Phylum Retaria Cavalier-Smith, 1999
Class Polycystinea Ehrenberg, 1839
Order Nassellaria Ehrenberg, 1876
Superfamily Eucyrtidioidea Ehrenberg, 1846, emend. Suzuki et al. (2021)
Family Eucyrtidiidae Ehrenberg, 1846, emend. Suzuki et al. (2021)
Genus *Cymaetron* Caulet, 1991

Type species.—*Cymaetron sinolampas* Caulet, 1991, p. 536, pl. 4, figs. 10–12; by monotypy.

Cymaetron? *dilatatus* new species
Figure 3.1–3.4

Holotype.—Figure 3.1; collection number USTL 3483-1; coordinates V46/2; sample ODP 1260A-9R-4W, 55–57 cm; upper part of the *Podocyrtis* (*L.*) *mitra* Zone, in the *Podocyrtis* (*P.*) *apeza* Subzone (late Lutetian, middle Eocene).

Diagnosis.—Trisegmented eucyrtidiid with an abdomen constricted in two false segments.

Occurrence.—This species occurs sporadically throughout the studied interval, from the upper part of the *Podocyrtis* (*P.*) *ampla* Zone, to the lower part of the *Podocyrtis* (*L.*) *goetheana* Zone.

Description.—Shell trisegmented, smooth and robust, with the collar and lumbar strictures marked externally by a change in the shell contour. Cephalis proportionally small, globular, poreless or bearing a few small circular pores. Apical spine extending outward as a strong apical tribladed horn longer than the cephalis, and dorsal spine prolonged as thoracic rib on upper thorax. Thorax truncate conical to slightly inflated conical, with subcircular pores, hexagonally framed and quincuncially arranged. Abdomen conspicuously inflated in its proximal part, usually 1.5–2 times as wide as thorax, then subcylindrical to truncate conical. The two parts of the abdomen are not subdivided into segments by an inner ring. Abdominal pores subcircular, hexagonally framed, and quincuncially arranged, sometimes less regularly arranged in the most distal part of the segment. Aperture open wide. Abdominal termination invariably ragged along a pore row.

Etymology.—The specific epithet refers to the expanded proximal part of the abdomen of the new species; *dilatatus* in Latin means 'dilated, expanded.' The specific epithet is to be treated as an adjective in the nominative singular.

Dimensions.—Based on 10 specimens (mean): total length without the apical horn 145–188 µm (176), length of apical horn 18–31 µm (24), length of cephalothorax without the apical horn 45–66 µm (56), length of abdomen 51–155 µm (117), maximum breadth of abdomen 82–129 µm (95).

Remarks.—*Cymaetron*? *dilatatus* n. sp. is tentatively assigned to the genus *Cymaetron* based on the characteristic undulated outline of the shell, which is constricted in false segments. However, the generic assignment is doubtful because the genus *Cymaetron* was originally described by Caulet (1991) as a two-segmented eucyrtidiid, while *C.*? *dilatatus* n. sp. clearly displays a trisegmented shell. In addition, *C.*? *dilatatus* n. sp. differs from *C. sinolampas* Caulet, 1991, the only other species of the genus, by having only one abdominal constriction. *Cymaetron*? *dilatatus* n. sp. also is distinguished from all other eucyrtidiid species with

https://doi.org/10.1017/jpa.2022.82 Published online by Cambridge University Press

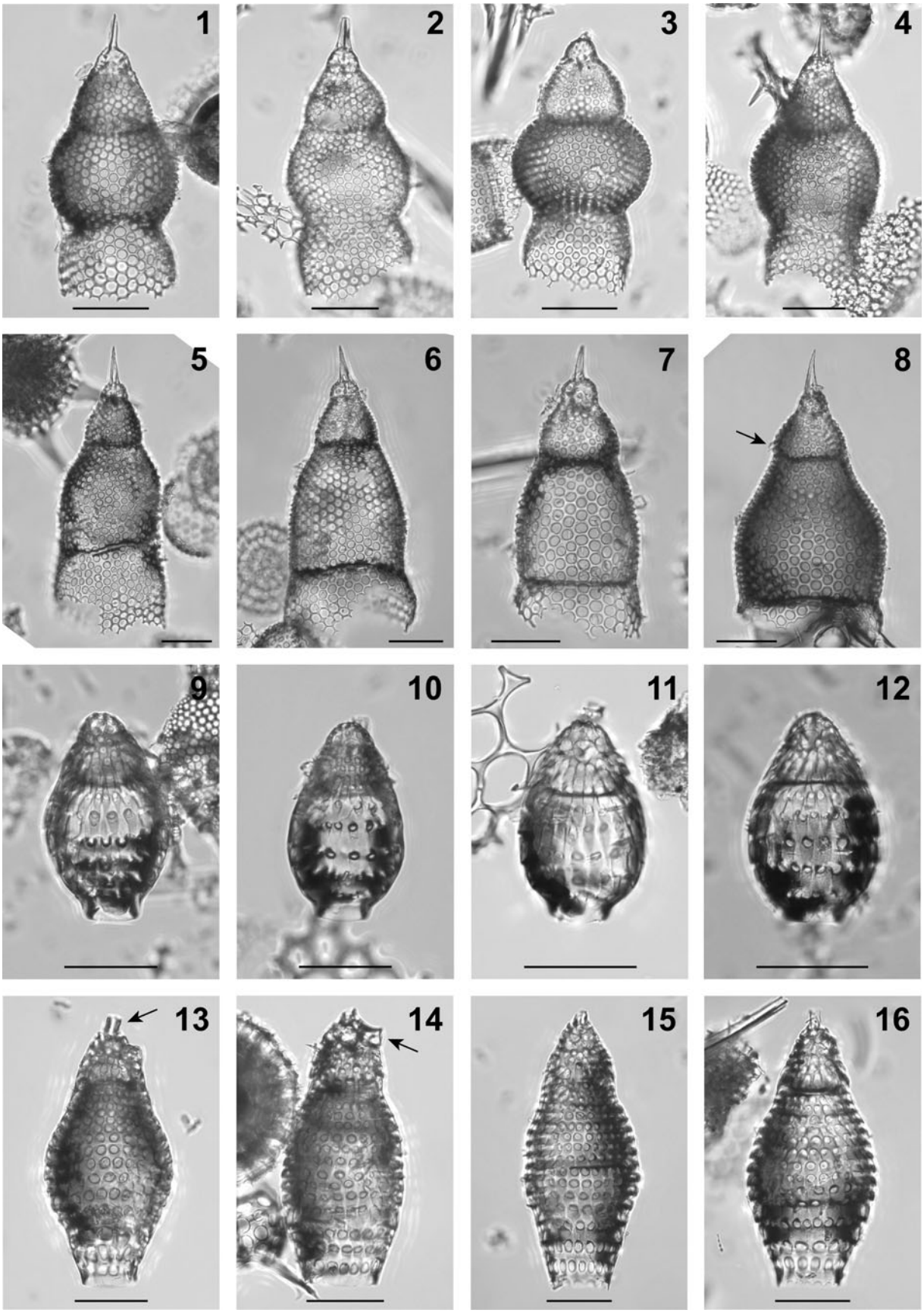

https://doi.org/10.1017/jpa.2022.82 Published online by Cambridge University Press

Figure 3. Composite light micrographs of new radiolarian species from ODP Site 1260 (Demerara Rise, western equatorial Atlantic). (**1–4**) *Cymaetron*? *dilatatus* n. sp.: (**1**) holotype, ODP 1260A-9R-4W, 55–57 cm, USTL 3483-1, V46/2; (**2**) ODP 1260A-9R-4W, 55–57 cm, USTL 3481-1, H41/3; (**3**) ODP 1260A-9R-3W, 55–57 cm, USTL 3479-1, T47/1 (mirrored); (**4**) ODP 1260A-9R-4W, 55–57 cm, USTL 3481-2, J37/2. (**5–8**) *Eucyrtidium levisaltatrix* n. sp.: (**5**) holotype, ODP 1260A-9R-4W, 55–57 cm, USTL 3482-1, J52/2; (**6**) ODP 1260A-9R-4W, 55–57 cm, USTL 3484-1, V45/2; (**7**) ODP 1260A-9R-3W, 55–57 cm, USTL 3478-1, E48/4; (**8**) specimen showing thoracic wing (arrow), ODP 1260A-8R-3W, 54–56 cm, USTL 3462-3, Z63/4 (mirrored). (**9–12**) *Dictyoprora curta* (Clark and Campbell): (**9**) ODP 1260A-14R-1W, 55–57 cm, USTL 3530-1, J40/1; (**10**) ODP 1260A-6R-3W, 55–57 cm, USTL 3424-1, H60/4; (**11**) ODP 1260A-9R-1W, 55–57 cm, USTL 2848-1, C46/2; (**12**) ODP 1260A-9R-1W, 55–57 cm, USTL 3473-1, L48/1. (**13–16**) *Spirocyrtis*? *renaudiei* n. sp.: (**13**) holotype, showing apical tube (arrow), ODP 1260A-8R-3W, 54–56 cm, USTL 3462-1, Q53/1 (mirrored); (**14**) specimen showing ventral tube (arrow), ODP 1260A-8R-3W, 54–56 cm, USTL 3462-2, L48/1 (mirrored); (**15**) ODP 1260A-7R-6W, 54–56 cm, USTL 3454-1, X45/2; (**16**) ODP 1260A-7R-6W, 54–56 cm, USTL 3454-2, R43/2. All scale bars equal 50 µm.

open abdomen in not having post-abdominal segments. Finally, *C*.? *dilatatus* n. sp. superficially resembles *Theocorys anaclasta* Riedel and Sanfilippo, 1970, from which it differs in having a much more elongated shell, a bladed apical horn, and smaller abdominal pores, which are regular in size.

Genus *Eucyrtidium* Ehrenberg, 1846

Type species.—*Lithocampe acuminata* Ehrenberg, 1844a, p. 84 (unfigured); Ehrenberg, 1854, pl. 22, fig. 27; subsequent designation by Frizzell and Middour (1951, p. 33).

Eucyrtidium levisaltatrix new species
Figure 3.5–3.8

Holotype.—Figure 3.5; collection number USTL 3482-1; coordinates J52/2; sample ODP 1260A-9R-4W, 55–57 cm; upper part of the *Podocyrtis* (*L.*) *mitra* Zone, in the *Podocyrtis* (*P.*) *apeza* Subzone (late Lutetian, middle Eocene).

Diagnosis.—*Eucyrtidium* species with an elongated abdomen, being the longer segment of the shell.

Occurrence.—This short-lived species is relatively rare from the uppermost part of the *Podocyrtis* (*L.*) *mitra* Zone, to the lower part of the *Podocyrtis* (*L.*) *chalara* Zone.

Description.—Shell multisegmented, conical-elongated, and thick-walled. Cephalis relatively small, globular, and sparsely pored, bearing a long conical apical horn. Collar stricture marked externally by a change in the shell contour. Thorax subspherical to campanulate, with circular pores quincuncially arranged. Dorsal spine of the initial spicule rarely protruding close to the thoracic stricture as a reduced, curved thoracic wing (Fig. 3.8). Abdomen subcylindrical to campanulate, being the longest segment. Abdominal pores circular, slightly bigger than thoracic ones, hexagonally framed, and longitudinally aligned. First post-abdominal segment proximally extended, with pores irregular in size and shape. Abdomen and first post-abdominal segment separated by a slight external constriction, and by a straight (Fig. 3.7) or wavy (Figs. 3.5, 3.6) internal ridge that appears externally as a thick obscure band. Distal part of the abdomen invariably ragged along a pore row.

Etymology.—From the Latin *levis*, meaning 'light, not heavy,' and *saltatrix*, meaning 'female dancer, dancing girl.' The specific epithet is to be treated as a noun in the nominative singular standing in apposition to the generic name.

Dimensions.—Based on six specimens (mean): total length without the apical horn 166–226 µm (194), length of apical horn 26–38 µm (30), length of cephalothorax 51–57 µm (55), length of abdomen 107–134 µm (119), maximum breadth of shell 101–127 µm (118).

Remarks.—This distinctive species is differentiated from all other middle Eocene *Eucyrtidium* species by its long apical horn, its well-marked abdominal stricture, and by its more conical shape due to elongation of the abdomen in comparison with other segments of the shell. Moreover, unlike other large species of the genus *Eucyrtidium*, the shell of *E. levisaltatrix* n. sp. is usually broken at the first post-abdominal segment.

It is likely that the new species originated from a stock of late middle Eocene multisegmented *Eucyrtidium* by elongation of its abdomen. However, further phylogenetic affinities remain unclear because *E. levisaltatrix* n. sp. appears suddenly in the fossil record.

Superfamily Artostrobioidea Riedel, 1967
Family Artostrobiidae Riedel, 1967, sensu Sugiyama (1998)
Genus *Dictyoprora* Haeckel, 1887

Type species.—*Dictyocephalus amphora* Haeckel, 1887, p. 1305, pl. 62, fig. 4; subsequent designation by Campbell (1953, p. 296).

Dictyoprora curta (Clark and Campbell, 1942)
Figure 3.9–3.12

1942 *Dictyocephalus* (*Dictyoprora*) *pulcherrimus curtus* Clark and Campbell, p. 79, pl. 8, figs. 3, 6, 7.
1973 *Theocampe pirum* (Ehrenberg); Foreman, p. 432, pl. 9, fig. 11 (part).
2005 *Dictyoprora* spp.; Nigrini et al., pl. P6, fig. 13.
2006 *Dictyoprora* sp. A; Funakawa et al., p. 18, pl. P2, fig. 10a, b.

Holotype.—Because no type was designated by Clark and Campbell (1942) in their original publication, any of the three illustrated specimens (pl. 8, figs. 3, 6, 7) are candidate lectotypes; they are all housed at the University of California, Museum of Paleontology.

Occurrence.—This species is found throughout the studied interval. It occurs sporadically from the *Thyrsocyrtis* (*P.*) *triacantha* Zone to the upper part of the *Podocyrtis* (*L.*) *mitra* Zone, and becomes more consistent and abundant from the upper part of the *Podocyrtis* (*L.*) *mitra* Zone to the *Podocyrtis* (*L.*) *goetheana* Zone.

https://doi.org/10.1017/jpa.2022.82 Published online by Cambridge University Press

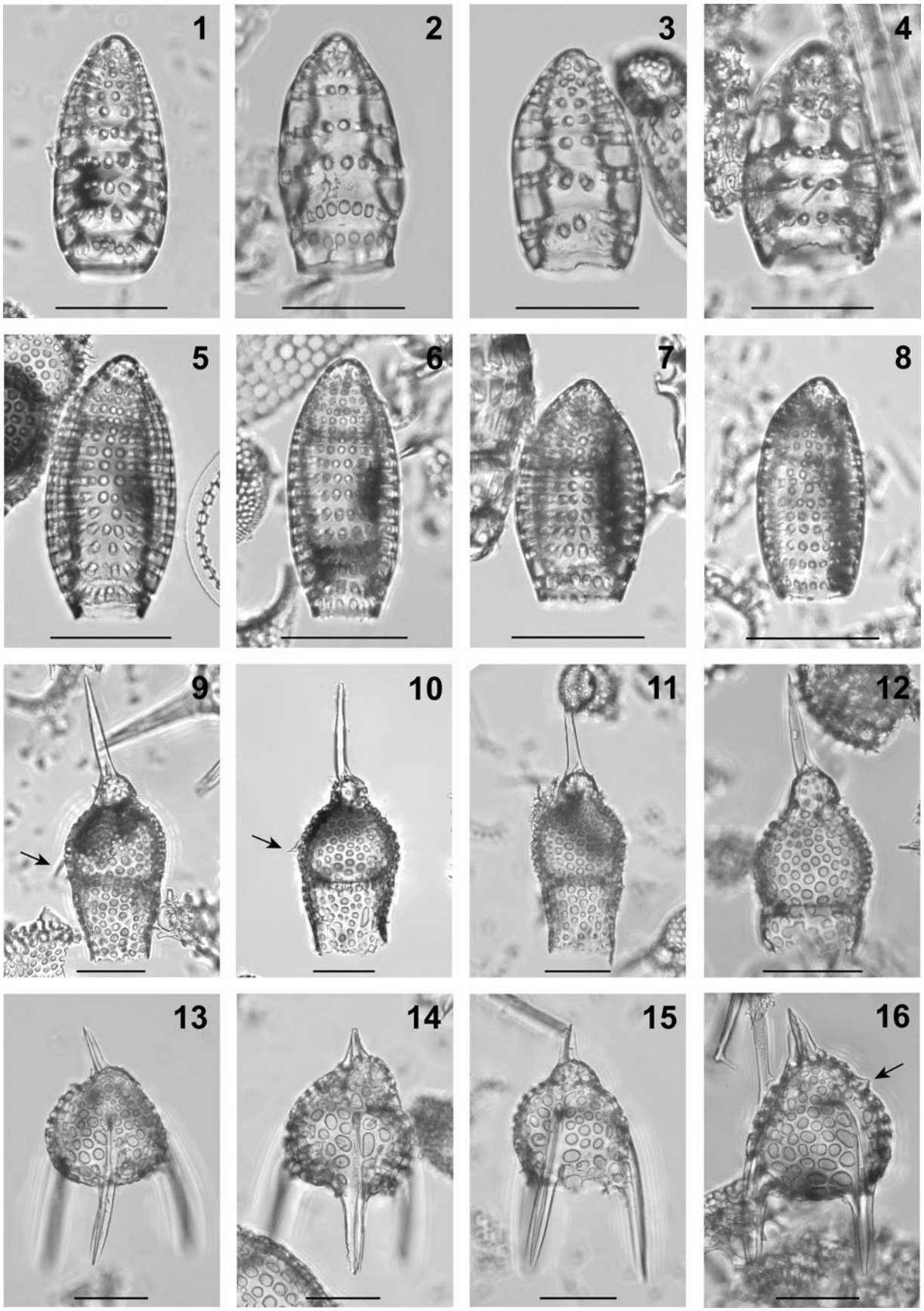

https://doi.org/10.1017/jpa.2022.82 Published online by Cambridge University Press

Figure 4. Composite light micrographs of radiolarian species from ODP Site 1260 (Demerara Rise, western equatorial Atlantic). (**1–4**) *Siphocampe pachyderma* (Ehrenberg): (**1**) ODP 1260A-9R-3W, 55–57 cm, USTL 3477-3, V50/3; (**2**) ODP 1260A-12R-6W, 55–57 cm, USTL 3519-1, F39/4; (**3**) ODP 1260A-11R-7W, 55–57 cm, USTL 3506-1, M43/3; (**4**) ODP 1260A-12R-4W, 55–57 cm, USTL 3514-1, S45/4. (**5–8**) *Siphocampe pollen* n. sp.: (**5**) holotype, ODP 1260A-13R-4W, 55–56 cm, USTL 2854-1, X67/4; (**6**) ODP 1260A-14R-1W, 55–57 cm, USTL 3530-3, N41/3; (**7**) ODP 1260A-10R-6W, 55–57 cm, USTL 3498-1, L52/2; (**8**) ODP 1260A-14R-1W, 55–57 cm, USTL 3531-1, W56/1. (**9–12**) *Pterocyrtidium eep* n. sp.: (**9**) holotype, showing thoracic wing (arrow), ODP 1260A-12R-CC, 63–177 cm, USTL 3521-1, U59/2 (mirrored); (**10**) specimen showing thoracic wing (arrow), ODP 1260A-12R-1W, 55–57 cm, USTL 2851-5, L64/3 (mirrored); (**11**) ODP 1260A-12R-CC, 63–177 cm, USTL 3521-2, U53/3; (**12**) ODP 1260A-12R-CC, 63–177 cm, USTL 3520-1, H36/3 (mirrored). (**13–16**) *Corythomelissa galea* (Ehrenberg) n. comb.: (**13**) ODP 1260A-11R-3W, 55–57 cm, USTL 3502-1, W34/4 (mirrored); (**14**) ODP 1260A-11R-4W, 55–57 cm, USTL 3503-1, F36/3 (mirrored); (**15**) ODP 1260A-11R-4W, 55–57 cm, USTL 3503-2, X39/3 (mirrored); (**16**) specimen showing sagittal horn (arrow), ODP 1260A-12R-CC, 63–177 cm, USTL 3520-2, X33/2 (mirrored). All scale bars equal 50 µm.

Description.—Ovoid shell made of three segments. Surface of the shell relatively smooth, but with fine surface sculpture on the abdomen. Cephalis hemispherical, unarmed, with scattered subcircular pores. Ventral pore large and circular, but no ventral tube develops. Collar stricture externally not defined in most of the observed specimens. Thorax truncate conical, with irregularly arranged circular pores. Lumbar stricture slightly expressed externally by a change in shell outline. Globular abdomen perforated by circular downward-directed pores arranged in 5–6 transverse rows. Each abdominal pore opens on a furrow dug within the wall thickness, which extends almost to the next pore row. Shell narrowing distally and ending in cylindrical poreless peristome with smooth margin.

Dimensions.—Based on 15 specimens (mean): total length 89–108 µm (97), length of cephalothorax 29–38 µm (34), length of abdomen 56–72 µm (63).

Remarks.—We have judged it appropriate to re-illustrate this species because it has been rarely reported since its original description by Clark and Campbell (1942) from upper middle Eocene strata of Mont Diablo, California. *Dictyoprora curta* is distinguished from all other dictyoprorids by its small globular abdomen (maximum length of abdomen <80 µm). This species also differs from *D. pirum* (Ehrenberg, 1874) and *D. gibsoni* (O'Connor, 1994) by having more closely spaced rows of pores, a well-developed peristome, and a thick-walled shell rather than a thin hyaline shell. *Dictyoprora curta* differs from *D. urceolus* (Haeckel, 1887) by its globular abdomen and its abdominal pores being downward directed, and differs from *D. armadillo* (Ehrenberg, 1874) and *D. ovata* (Haeckel, 1887) in lacking a cephalic horn and in having fewer than seven rows of abdominal pores. It is finally distinguished from *D. mongolfieri* (Ehrenberg, 1854) by not having abdominal pores aligned longitudinally and from *D. amphora* (Haeckel, 1887) by having abdominal pores that are uniform and aligned in transverse rows.

Genus *Siphocampe* Haeckel, 1882

Type species.—*Siphocampe annulosa* Haeckel, 1887, p. 1500, pl. 79, fig. 10; subsequent designation by Strelkov and Lipman (1959, p. 459).

Siphocampe pachyderma (Ehrenberg, 1874)
Figure 4.1–4.4

1874 *Eucyrtidium pachyderma* Ehrenberg, p. 231.
1876 *Eucyrtidium pachyderma*; Ehrenberg, p. 72, pl. 11, fig. 21.
1882b *Lithomitra pachyderma*; Bütschli, pl. 30, fig. 26.
1991 *Siphocampe pachyderma*; Caulet, p. 539, pl. 3, fig. 12.
2009 *Eucyrtidium pachyderma*; Ogane et al., pl. 21, fig. 1a–d.

Lectotype.—No holotype was designated by Ehrenberg in the original description of the species. The specimen drawn by Ehrenberg (1876, pl. 11, fig. 21) was re-illustrated by Ogane et al. (2009, pl. 21, fig. 1a–d) during their reexamination of Ehrenberg's collection, which is kept in the Museum für Naturkunde, Humboldt University (Berlin, Germany), and subsequently designated as a lectotype by O'Dogherty et al. (2021, p. 976).

Diagnosis.—Very thick-walled *Siphocampe* species, with an asymmetrically placed cephalis and widely spaced rows of abdominal pores.

Occurrence.—The record of this species is punctuated throughout the studied interval, from the *Thyrsocyrtis* (*P.*) *triacantha* Zone to the *Podocyrtis* (*L.*) *goetheana* Zone.

Description.—Three-segmented, small, spindle-shaped, and very thick-walled shell. Cephalis hemispherical to subspherical, asymmetrically placed, poreless or penetrated by a few subcircular pores. Ventral pore present, but ventral tube not developed. Absence of an apical horn. Collar and lumbar stricture indistinct in most of the observed specimens. Thorax trapezoidal, with 2–4 transverse rows of circular pores. Thoracic wall thickening distally. Abdomen elongated, subcylindrical to barrel-shaped, and very thick-walled, 2–3 times longer than the thorax. Abdominal pores small, circular, with tubular projections through the abdominal wall, arranged in 3–5 transverse rows of pores. Although the abdomen is smooth externally, internal indentations can be distinguished by transparency, the maximum thickness of the abdominal wall being reached between the rows of pores. Shell ending in a smooth poreless peristome.

Dimensions.—Based on six specimens (mean): total length: 84–119 µm (99), maximum breadth 43–57 µm (51).

Remarks.—*Siphocampe pachyderma* differs from all other species of the genus *Siphocampe* by its very thick-walled and almost hyaline shell, and from *Plannapus aitai* O'Connor, 2000, in having a less-elongated shell, with fewer than 10 transverse rows of pores.

https://doi.org/10.1017/jpa.2022.82 Published online by Cambridge University Press

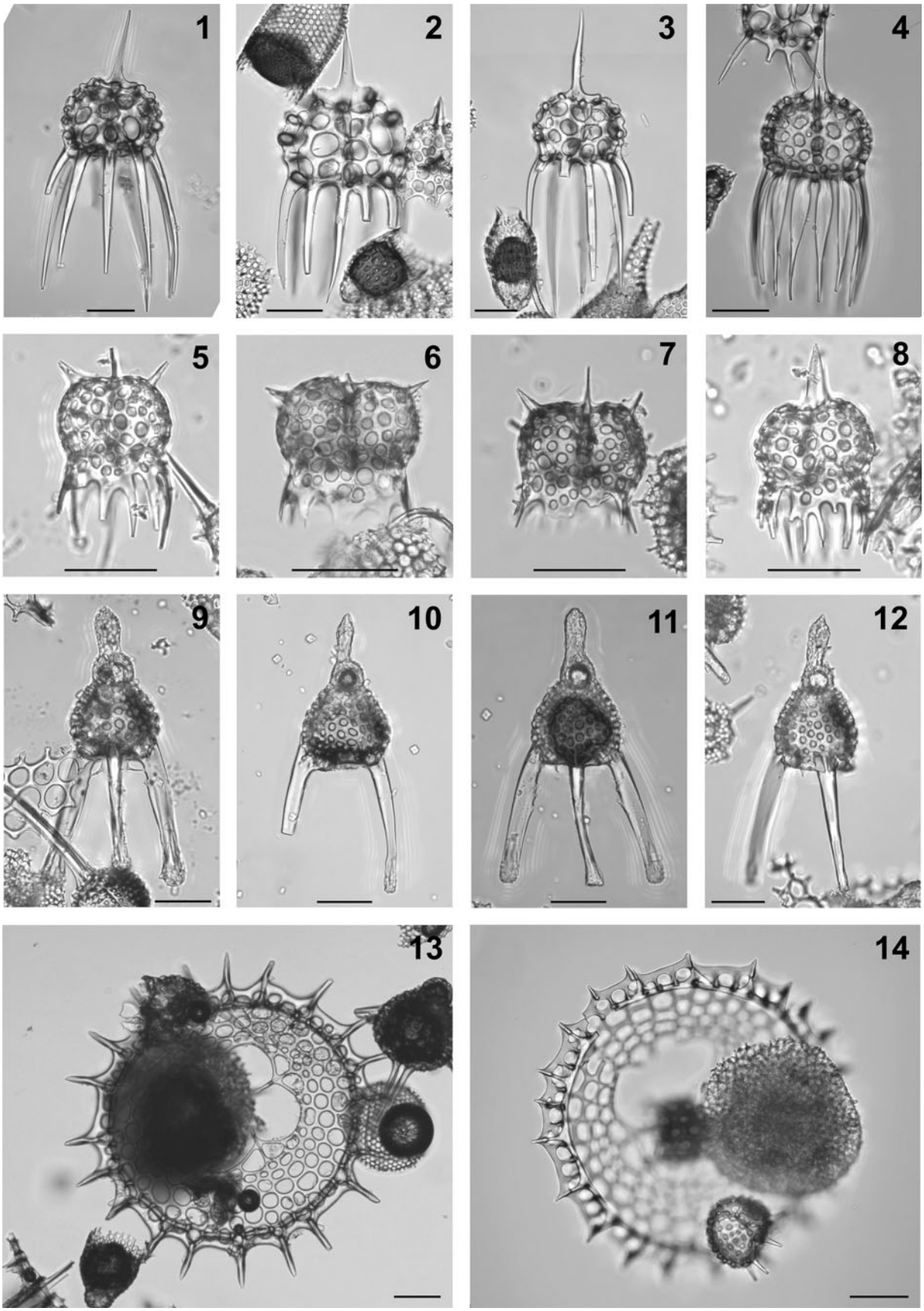

https://doi.org/10.1017/jpa.2022.82 Published online by Cambridge University Press

Figure 5. Composite light micrographs of radiolarian species from ODP Site 1260 (Demerara Rise, western equatorial Atlantic). (**1–3**) *Petalospyris cometa* n. sp.: (**1**) holotype, ODP 1260A-6R-2W, 55–57 cm, USTL 3421-1, W42/3; (**2**) ODP 1260A-6R-1W, 55–57 cm, USTL 2847-1, X45/1; (**3**) ODP 1260A-6R-1W, 55–57 cm, USTL 2847-2, D39/2. (**4**) *Petalospyris argiscus* Ehrenberg, 1874: ODP 1260A-13R-4W, 55–56 cm, USTL 2854-4, M38/4. (**5–7**) *Petalospyris castanea* n. sp.: (**5**) holotype, ODP 1260A-9R-3W, 55–57 cm, USTL 3477-1, H33/3; (**6**) ODP 1260A-8R-2W, 54–56 cm, USTL 3461-1, R55/3; (**7**) ODP 1260A-9R-3W, 55–57 cm, USTL 3479-2, S42/1**.** (**8**) *Petalospyris confluens* Ehrenberg, 1874: ODP 1260A-9R-3W, 55–57 cm, USTL 3478-3, U43/3. (**9–12**) *Lychnocanium nimrodi* n. sp.: (**9**) holotype, ODP 1260A-9R-4W, 55–57 cm, USTL 3483-2, L38/2; (**10**) ODP 1260A-9R-4W, 55–57 cm, USTL 3481-4, U38/3 (mirrored); (**11**) ODP 1260A-9R-4W, 55–57 cm, USTL 3484-2, L36/9; (**12**) ODP 1260A-9R-2W, 55–57 cm, USTL 3474-2, O38/3. (**13, 14**) *Velicucullus armatus* n. sp.: (**13**) holotype, ODP 1260A-14R-5W, 55–57 cm, USTL 3277-1, Q41/1; (**14**) ODP 1260A-13R-4W, 55–56 cm, USTL 2854-3, T61/3. All scale bars equal 50 µm.

Siphocampe pollen new species
Figure 4.5–4.8

1975 *Theocampe amphora* group Chen, p. 456, pl. 2, fig. 2 (part).

Holotype.—Figure 4.5; collection number USTL 2854-1; coordinates L48/1; sample 1260A-13R-4W, 55–56 cm; lowermost part of the *Podocyrtis* (*L.*) *mitra* Zone, in the *Artostrobus quadriporus* Subzone (late Lutetian, middle Eocene).

Diagnosis.—*Siphocampe* species with a symmetrically placed cephalis and thick-walled abdomen with closely spaced transverse rows of pores.

Occurrence.—*Siphocampe pollen* n. sp. is found in almost all the studied samples, from the lowermost part of the *Podocyrtis* (*P.*) *ampla* Zone, to the lower part of the *Podocyrtis* (*L.*) *goetheana* Zone.

Description.—Shell of three segments, spindle-shaped, and smooth-surfaced. Cephalis hemispherical, asymmetrically placed, and partially embedded in the thorax. Absence of an apical horn. Ventral pore present, but ventral tube not developed. Cephalic pores subcircular, sparse, and irregularly arranged. Collar stricture slightly obscure externally, but not marked by a change in the shell contour. Thorax truncate conical with 5–6 closely spaced transverse rows of small subcircular to circular pores. Lumbar stricture usually obscure externally. Abdomen elongated, barrel-shaped, and thick-walled, about twice the length of the cephalothorax. Abdominal pores small, circular, cylindrical, arranged in 9–10 transverse rows. Distal part of the abdomen usually ragged (Fig. 4.6, 4.7), but on complete specimens the termination of the shell is a thin annular poreless peristome (Fig. 4.5).

Etymology.—From the Latin *pollen* meaning 'flour flower,' for its resemblance to a pollen grain (i.e., the male reproductive particles produced by the anther lodges of flower stamens). The specific epithet is to be treated as a noun in the nominative singular standing in apposition to the generic name.

Dimensions.—Based on 24 specimens (mean): total length 68–129 µm (91), maximum breadth 30–55 µm (45).

Remarks.—The general form of the shell of *Siphocampe pollen* n. sp. resembles those of *S. acephala* (Ehrenberg, 1874) and *S. missilis* O'Connor, 1994. It differs from these species in having a thicker abdominal and thoracic wall, and 9–10 transverse rows of pores on the abdomen, instead of 4–8 rows for *S. acephala* and 8–17 rows for *S. missilis*. The new species also differs from *S. acephala* in having a spindle-shape rather than subcylindrical abdomen, and from *S. missilis* in having an asymmetrical cephalis. It differs from *S. imbricata* (Ehrenberg, 1874), *S. lineata* (Ehrenberg, 1839), and *S. arachnea* (Ehrenberg, 1862) by the smaller length of its abdomen and in lacking abdominal indentations. The new species is distinguished from the co-occurring species *S. pachyderma* (Ehrenberg, 1874) by having a thinner abdominal wall and closely spaced transverse rows of pores on the abdomen. Finally, *S. pollen* n. sp. differs from the enigmatic *Plannapus*? *aitai* O'Connor, 2000, in having an asymmetrically placed cephalis that never bears an apical horn, and a trisegmented shell with thinner walls.

Siphocampe pollen n. sp. is probably related to *S. acephala* and *S. pachyderma*, which also have an asymmetrical cephalis. The characteristic thickness of the shell wall also suggests a close proximity between the *S. pollen* n. sp. and *S. pachyderma*.

Genus *Spirocyrtis* Haeckel, 1882, emend. Nigrini (1977)

Type species.—*Spirocyrtis scalaris* Haeckel, 1887, p. 1509, pl. 76, fig. 14; subsequent designation by Campbell (1954, p. D142).

Spirocyrtis? *renaudiei* new species
Figure 3.13–3.16

Holotype.—Figure 3.13; collection number USTL 3462-1; coordinates Q53/1; sample ODP 1260A-8R-3W, 54–56 cm; *Podocyrtis* (*L.*) *chalara* Zone, in the *Rhopalosyringium*? *biauritum* Subzone (late Lutetian, middle Eocene).

Diagnosis.—Artostrobiid with a multisegmented pupoid shell, a short truncated apical tube and a flared ventral tube.

Occurrence.—From the uppermost part of the *Podocyrtis* (*L.*) *mitra* Zone, to the lowermost part of the *Podocyrtis* (*L.*) *goetheana* Zone.

Description.—Shell pupoid to spindle-shaped, thick-walled, and multisegmented, fourth segment being the widest (rarely the third). Strictures usually indistinct or just slightly obscure externally. Cephalis truncate conical, with downward-directed subcircular pores, bearing a short truncated apical tube (Fig. 3.13) and a robust, distally flared ventral tube that opens almost at a right angle to the axis of the shell (Fig. 3.14). Thorax truncate conical, half the length of the cephalis, with 2–4 transverse rows of subcircular pores. Abdomen truncate conical or slightly campanulate, longer than thorax, bearing

https://doi.org/10.1017/jpa.2022.82 Published online by Cambridge University Press

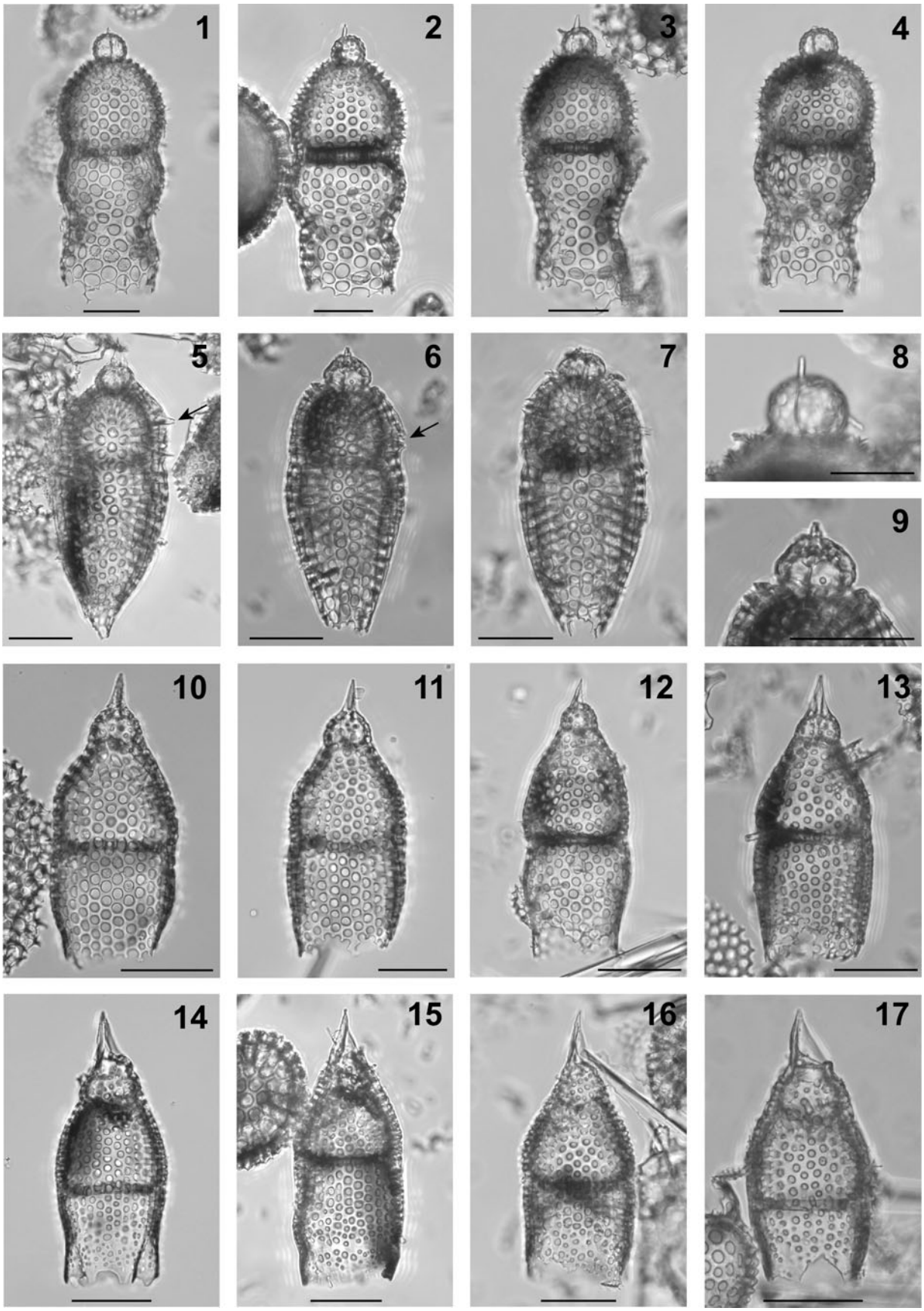

https://doi.org/10.1017/jpa.2022.82 Published online by Cambridge University Press

Figure 6. Composite light micrographs of new radiolarian species from ODP Site 1260 (Demerara Rise, western equatorial Atlantic). (**1–4**, **8**) *Aphetocyrtis zamenhofi* n. sp.: (**1**) holotype, ODP 1260A-15R-2W, 55–57 cm, USTL 3543-1, Q37/4; (**2**) ODP 1260A-14R-CC, 63–117 cm, USTL 3540-1, P37/1; (**3**) ODP 1260A-15R-1W, 55–57 cm, USTL 3541-1, N47/2; (**4**) ODP 1260A-15R-1W, 55–57 cm, USTL 3541-2, Q54/1; (**8**) focus on the cephalis, ODP 1260A-15R-2W, 55–57 cm, USTL 3543-2. (**5–7**, **9**) *Aphetocyrtis*? *columboi* n. sp.: (**5**) holotype, showing thoracic wing (arrow), ODP 1260A-6R-6W, 55–57 cm, USTL 3438-1, J31/1; (**6**) specimen showing thoracic wing (arrow), ODP 1260A-6R-6W, 55–57 cm, USTL 3438-2, G46/1; (**7**) ODP 1260A-6R-6W, 55–57 cm, USTL 3438-3, L38/3; (**9**) focus on the cephalis of the specimen illustrated as Figure 6.6. (**10–13**) *Aphetocyrtis*? *spheniscus* n. sp.: (**10**) holotype, ODP 1260A-12R-1W, 55–57 cm, USTL 2851-2, Y49/1; (**11**) ODP 1260A-9R-3W, 55–57 cm, USTL 3478-2, S52/4; (**12**) ODP 1260A-12R-1W, 55–57 cm, USTL 2851-3, G45/2 (mirrored); (**13**) ODP 1260A-12R-3W, 55–57 cm, USTL 3512-2, H58/1. (**14–17**) *Albatrossidium regis* n. sp.: (**14**) holotype, ODP 1260A-12R-1W, 55–57 cm, USTL 2851-1, Y54/2 (mirrored); (**15**) ODP 1260A-13R-5W, 54–56 cm, USTL 3525-1, W56/2 (mirrored); (**16**) ODP 1260A-14R-1W, 55–57 cm, USTL 3530-2, M38/1 (mirrored); (**17**) ODP 1260A-12R-5W, 55–57 cm, USTL 3516-1, N49/1 (mirrored). All scale bars equal 50 µm.

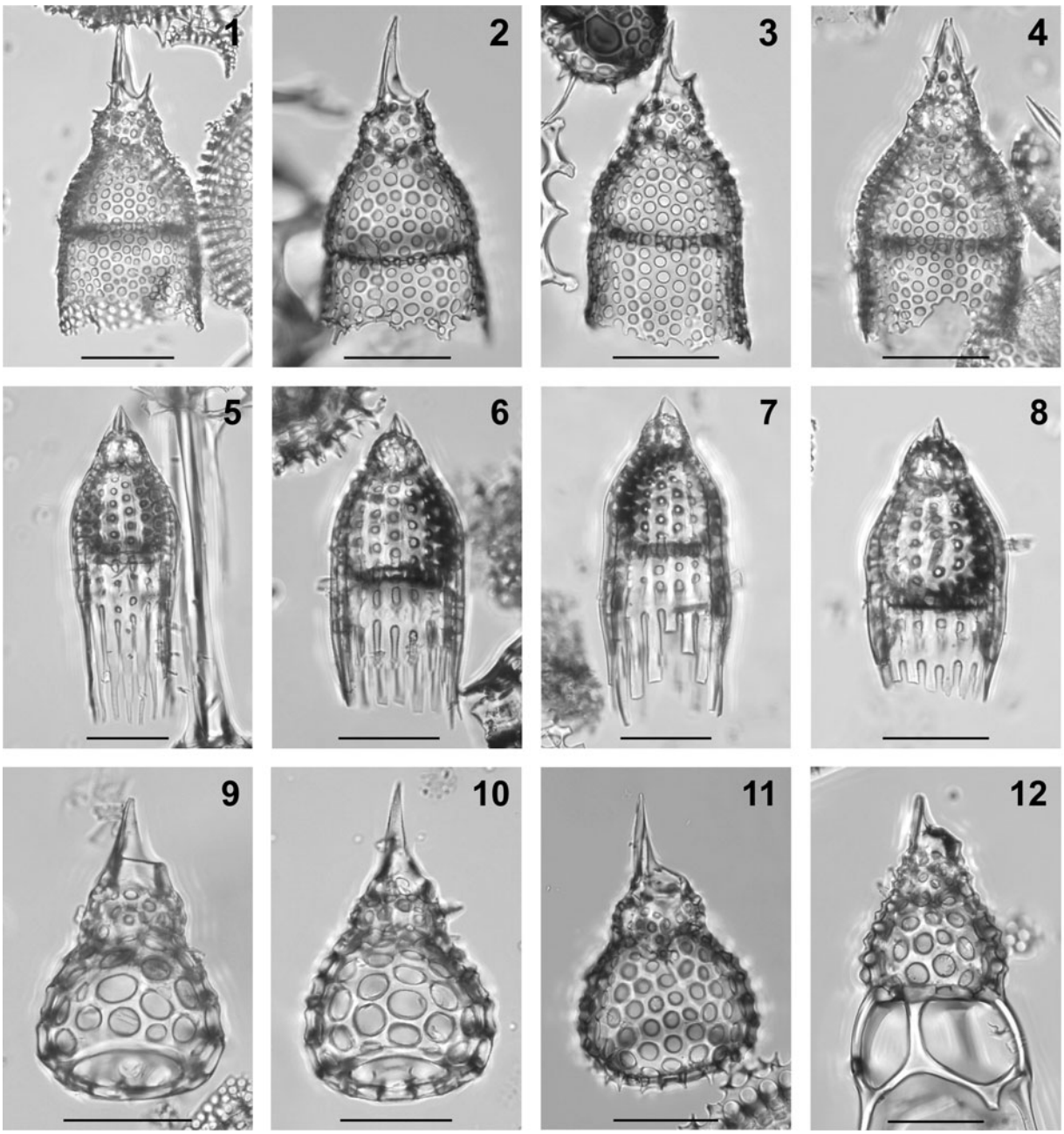

Figure 7. Composite light micrographs of radiolarian species from ODP Site 1260 (Demerara Rise, western equatorial Atlantic). (**1–4**) *Albatrossidium annikasanfilippoae* n. sp.: (**1**) holotype, ODP 1260A-12R-3W, 55–57 cm, USTL 3512-1, Y39/1; (**2**) ODP 1260A-13R-4W, 55–57 cm, USTL 2854-5, X67/4; (**3**) ODP 1260A-13R-4W, 55–57 cm, USTL 2854-2, O66/1; (**4**) ODP 1260A-9R-3W, 55–57 cm, USTL 3477-2, L56/3. (**5–8**) *Phormocyrtis lazari* n. sp.: (**5**) holotype, ODP 1260A-9R-2W, 55–57 cm, USTL 3474-1, T40/4; (**6**) ODP 1260A-9R-3W, 55–57 cm, USTL 3480-1, M35/1; (**7**) ODP 1260A-9R-4W, 55–57 cm, USTL 3482-2, W36/3; (**8**) ODP 1260A-9R-4W, 55–57 cm, USTL 3481-3, E38/3. (**9–12**) *Podocyrtis* (*Lampterium*) *puellasinensis* Ehrenberg, 1874: (**9**) ODP 1260A-6R-2W, 55–57 cm, USTL 3420-1, U56/1; (**10**) ODP 1260A-9R-4W, 55–57 cm, USTL 3484-3, D47/3; (**11**) ODP 1260A-12R-1W, 55–57 cm, USTL 2851-4, C47/4 (mirrored). (**12**) *Podocyrtis* (*Lampterium*) *goetheana* (Haeckel, 1887), focus on the cephalothorax, ODP 1260A-8R-2W, 54–56 cm, USTL 3461-2, S49/1 (mirrored). All scale bars equal 50 µm.

https://doi.org/10.1017/jpa.2022.82 Published online by Cambridge University Press

3–5 transverse pore rows. First post-abdominal segment short, cylindrical and medially expanded, with its lower margin marked by a narrow hyaline band. Other post-abdominal segments short, truncate conical, wider proximally than distally. All post-abdominal segments with subcircular pores arranged in 1–3 transverse rows. Pores tend to be larger distally. Last segment terminating in narrow hyaline peristome (Fig. 2.1, 2.2), ragged in most of the observed specimens.

Etymology.—This species is named after Dr. Johan Renaudie (Museum für Naturkunde, Humboldt-Universität, Berlin), in honor of his contribution to the study of Cenozoic radiolarians. The specific epithet is to be treated as a noun in the genitive case formed from a modern personal name.

Dimensions.—Based on 20 specimens (mean): total length without the apical tube 173–216 µm (192), maximum breadth of shell 66–98 µm (89), length of apical tube 9–13 µm (10).

Remarks.—*Spirocyrtis*? *renaudiei* n. sp. differs from all other *Spirocyrtis* species in having a pupoid rather than a conical shell. The new species is also distinguished from *Botryostrobus grantmackiei* (O'Connor, 1997a) and *B. hollisi* (O'Connor, 1997a) in having bigger pores arranged in more closely spaced transverse rows, and in not having post-abdominal indentations. *Spirocyrtis*? *renaudiei* n. sp. is distinguished from *B. miralestensis* (Campbell and Clark, 1944) and *B. aquilonaris* (Bailey, 1856) in being more elongated and in lacking a hyaline peristome, and from *B. bramlettei* (Campbell and Clark, 1944), *B. auritus* (Ehrenberg, 1844a), and *B. australis* (Ehrenberg, 1844b) in having less-rounded abdominal and post-abdominal segments, and in lacking hyaline bands between post-abdominal segments.

The generic assignment of *S.*? *renaudiei* n. sp. is uncertain because of its affinity to both *Botryostrobus* and *Spirocyrtis*. On the one hand, it appears to be close to the genus *Botryostrobus* by the general shape of its shell, which is characterized by a pupoid shape narrowing distally, and by the fact that the test is widest at or before the fifth segment (O'Connor, 1997a). On the other hand, *S.*? *renaudiei* n. sp. differs from all *Botryostrobus* species in bearing a short apical tube and a distally flared ventral tube, which are two diagnostic characters of the genus *Spirocyrtis* (Nigrini, 1977). The oldest known representatives of both genera have been found in upper Paleocene to lower Oligocene sequences: *B. joides* Petrushevskaya, 1975 (upper Eocene–lower Oligocene), *S.*? *hollisi* Renaudie and Lazarus, 2012 (upper Paleocene, see Hollis, 2002), *S. greeni* O'Connor, 1999a (upper Eocene), and *S. proboscis* O'Connor, 1994 (lower Oligocene). The middle Eocene *S.*? *renaudiei* n. sp. represents therefore one of the oldest species of the genus *Spirocyrtis*, and the mixture of features observed in this species may indicate that it is very close to the divergence between the genera *Botryostrobus* and *Spirocyrtis*.

Family Rhopalosyringiidae Empson-Morin, 1981
Genus *Pterocyrtidium* Bütschli, 1882a

Type species.—*Pterocanium barbadense* Ehrenberg, 1874, p. 254 (unfigured); Ehrenberg, 1876, p. 82, pl. 17, fig. 6; subsequent designation by Petrushevskaya and Kozlova (1972, p. 552).

Pterocyrtidium eep new species
Figure 4.9–4.12

Holotype.—Figure 4.9; collection number USTL 3521-1; coordinates U59/2; sample ODP 1260A-12R-CC, 63–177 cm; lower part of the *Podocyrtis* (*L.*) *mitra* Zone, in the *Artostrobus quadriporus* Subzone (Lutetian, middle Eocene).

Diagnosis.—*Pterocyrtidium* species with a long apical horn, and a roundish thorax larger than the abdomen.

Occurrence.—Rare, from the uppermost part of the *Podocyrtis* (*P.*) *ampla* Zone to the upper part of the *Podocyrtis* (*L.*) *mitra* Zone.

Description.—Three-segmented, subcylindrical shell. Cephalis relatively small and globular, penetrated with a few subcircular pores and bearing a remarkably strong apical horn, usually three times as long as the cephalis height. Two dimples present at the base of the apical horn (Fig. 4.9). Collar stricture expressed externally as a constriction. Thorax roundish to inflated, penetrated by numerous subcircular pores quincuncially arranged and hexagonally framed. In some specimens, primary lateral spines growing out from the lower thorax as one or two sharply pointed lateral wings (Fig. 4.9, 4.10). Lumbar stricture marked by a change in the shell contour and a thick internal ridge. Abdominal pores subcircular and roughly aligned in longitudinal rows, and less numerous in the distal part of the abdomen. Aperture open and bordered by a hyaline band, or ragged along a pore row.

Etymology.—The specific epithet is to be treated as an arbitrary combination of letters derived from the acronym used to designate the Evolution, Ecology, Paleontology (EEP) Laboratory of the University of Lille, as a token of gratitude for the assistance offered to the first author.

Dimensions.—Based on five specimens (mean): total length without the apical horn 133–153 µm (138), length of apical horn 61–75 µm (70), length of cephalothorax without the apical horn 76–84 µm (79), length of abdomen 54–71 µm (58).

Remarks.—*Pterocyrtidium eep* n. sp. is distinguished from *P. barbadense* (Ehrenberg, 1874) and *P. praebarbadense* Kozlova, 1983, by its long sharply pointed apical horn, and from *P. borisenkoi* Nishimura, 1992, by possessing a roundish thorax instead of a pyramidal thorax. The new species differs also from *P. genrietta* Nishimura, 1992, by having a longer apical horn, and a thorax wider than the abdomen. Finally, *P. eep* n. sp. differs from *P. zitteli* Bütschli, 1882b, by having a simple, conical apical horn rather than a dichotomous, bladed apical horn, and by the absence of a ventral horn on the cephalis. Finally, the new species is distinguished from similarly shaped upper Paleogene pterocorythids in having an unilobed cephalis.

https://doi.org/10.1017/jpa.2022.82 Published online by Cambridge University Press

Superfamily Acanthodesmioidea Haeckel, 1862
Family Cephalospyrididae Haeckel, 1882
Genus *Petalospyris* Ehrenberg, 1846

Type species.—*Petalospyris diaboliscus* Ehrenberg, 1847, p. 55, fig. 6; by monotypy.

Petalospyris cometa new species
Figure 5.1–5.3

Holotype.—Figure 5.1; collection number USTL 3421-1; coordinates W42/3; sample ODP 1260A-6R-2W, 55–57 cm; lower part of the *Podocyrtis* (*L.*) *goetheana* Zone (early Bartonian, middle Eocene).

Diagnosis.—Spyrid with a tuberculate shell, big cephalic pores, and nine conical feet.

Occurrence.—*Petalospyris cometa* n. sp. appears in the lowermost part of the *Podocyrtis* (*L.*) *goetheana* Zone at ODP Site 1260.

Description.—Lattice shell tuberculate, thick-walled, with slight external sagittal stricture, and not extending below the basal ring. Sagittal ring D-shaped. Apical horn robust, triangular, variable in length, generally less than half the height of the lattice shell. Cephalic pores subcircular to quadrate, unequal in size, and arranged in symmetry with respect to the sagittal stricture. Vertical pore present, showing a strong vertical spine. Presence of nine conical feet with pointed end, emerging directly from the basal ring. All feet well-individualized, straight or slightly divergent, with most of the curvature proximal.

Etymology.—From the Latin *cometa*, meaning 'comet.' The specific epithet is to be treated as a noun in the nominative singular standing in apposition to the generic name.

Dimensions.—Based on 15 specimens (mean): length of cephalis without the apical horn 74–100 µm (86), maximum breadth of cephalis 104–132 µm (118), length of apical horn 33–85 µm (62), length of lamellar feet 70–180 µm (129).

Remarks.—*Petalospyris cometa* n. sp. differs from all *Dorcadospyris* species and from *Dendrospyris stylophora* (Ehrenberg, 1874) in having nine lamellar feet emerging from the basal ring, instead of a reduced number of curved or straight feet that are round in cross section. Representatives of *Petalospyris cometa* n. sp. differ from those of *P. confluens* Ehrenberg, 1874, in having bigger cephalic pores, and long and well-individualized lamellar feet (Fig. 5.8). *Petalospyris cometa* n. sp. differs from *P. inferispina* (Goll, 1968), *P. flabellum* Ehrenberg, 1874, *P. platyacantha* Ehrenberg, 1974, and *Elaphospyris*? *golli* (Nishimura, 1992) in having larger pores, a rougher surface, and an apical horn that is shorter than the lattice shell. *Petalospyris cometa* n. sp. also differs from *P. diaboliscus* Ehrenberg, 1847, and *P. castanea* n. sp. by the absence of two lateral spines on the cephalis. Finally, *P. cometa* n. sp. is distinguished from *P. argiscus* Ehrenberg, 1874 (Fig. 5.4), *P. carinata* Ehrenberg, 1874, and *P. eupetala* Ehrenberg, 1874, by having fewer than 10 pores on the circumference of the cephalis at its widest part, a robust apical horn that is shorter than the lattice shell, and by having a wide vertical pore.

The origin of *P. cometa* n. sp. is to be found within a number of middle Eocene *Petalospyris* species displaying a pebbly surfaced cephalis and numerous teeth surrounding the cephalic aperture, introduced by Ehrenberg (1874) as distinct species: *P. argiscus*, *P. carinata*, and *P. eupetala*. *Petalospyris argiscus* is abundant throughout the studied interval, displaying a high intraspecific variability, both in the expression of the sagittal constriction and in the length and inclination of the lamellar teeth. At ODP Site 1260, we also observed specimens with proximally carinate lamellar teeth, especially in the *Podocyrtis* (*L.*) *mitra* Zone. All these different morphotypes do not form homogeneous groups that are distinct from typical *P. argiscus* (Fig. 5.4); we therefore chose to include them all under this species. Thus, because our enlarged concept of *P. argiscus* encompasses morphotypes previously assigned to *P. eupetala* and *P. carinata*, the latter are here considered as synonyms of *P. argiscus*. In this revised taxonomic framework, *P. cometa* n. sp. is regarded as an offshoot of *P. argiscus* (Fig. 8).

Petalospyris castanea new species
Figure 5.5–5.7

Holotype.—Figure 5.5; collection number USTL 3477-1; coordinates H33/3; sample ODP 1260A-9R-3W, 55–57 cm; upper part of the *Podocyrtis* (*L.*) *mitra* Zone, in the *Podocyrtis* (*P.*) *apeza* Subzone (late Lutetian, middle Eocene).

Diagnosis.—Spyrid with two lateral spines on the cephalis and a latticed thorax terminating in long teeth.

Occurrence.—This species occurs sporadically from the upper part of the *Podocyrtis* (*L.*) *mitra* Zone, until the end of the studied interval, which falls in the lowermost part of the *Podocyrtis* (*L.*) *goetheana* Zone.

Description.—Shell dicyrtid, smooth, with a bilobed cephalis and a short latticed thorax. Cephalis globular, separated into two lobes by a weak sagittal constriction, bearing a short needle-like apical horn and two short lateral spines. Lateral spines developed directly from the latticed shell. Cephalic and thoracic pores subcircular, of different sizes, and randomly distributed. Thorax terminating in a ring of teeth as long as the thorax or a little longer (usually broken), pointing distally and slightly curved inward.

Etymology.—From the Latin *castanea*, meaning 'chestnut,' for its resemblance to the fruit of the sweet chestnut tree. The specific epithet is to be treated as an adjective in the nominative singular.

Dimensions.—Based on five specimens (mean): length of cephalis without the apical horn 33–45 µm (40), maximum

https://doi.org/10.1017/jpa.2022.82 Published online by Cambridge University Press

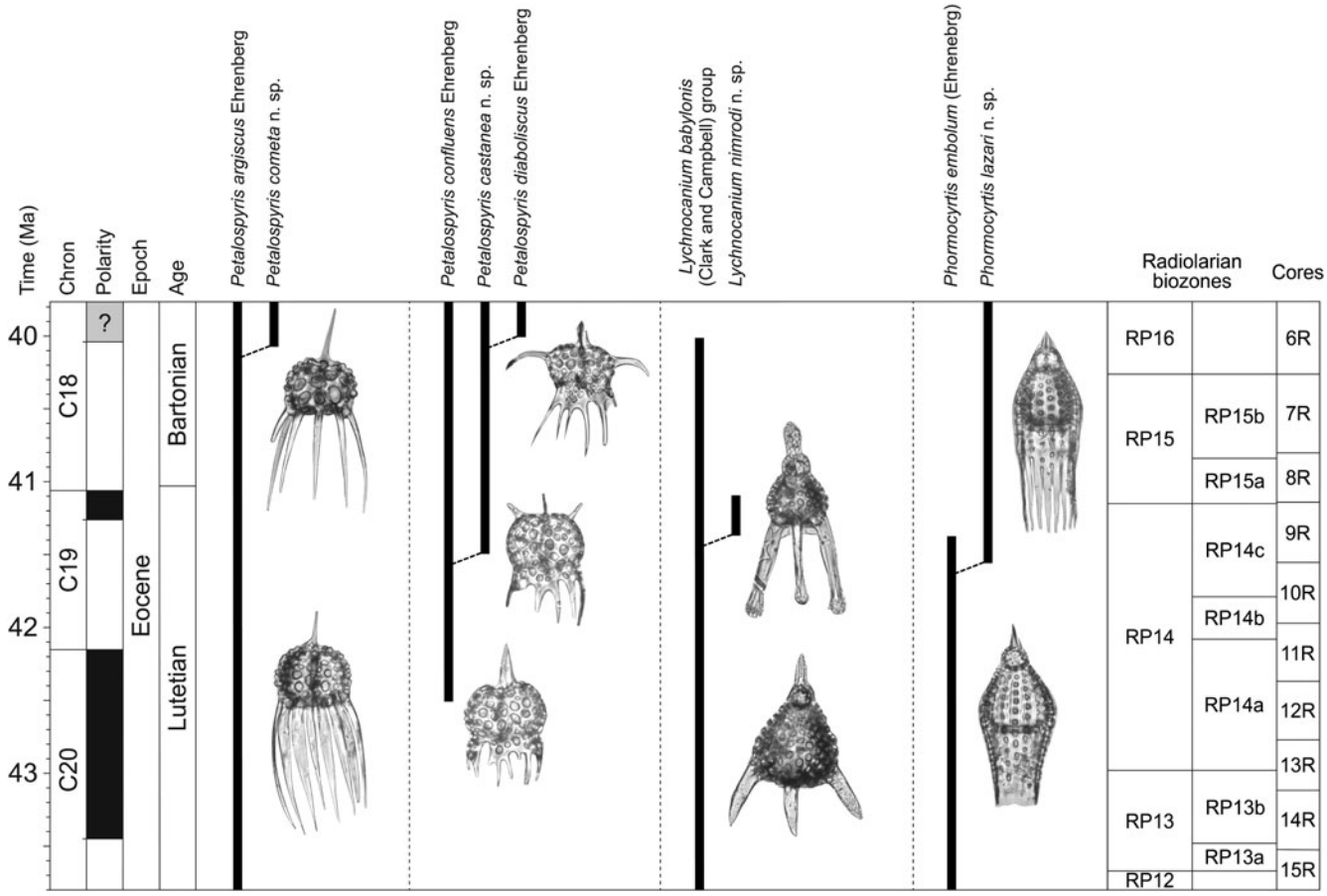

Figure 8. Stratigraphic ranges and evolutionary relationships to previously described species of four of the new species described at ODP Site 1260 (Demerara Rise, western equatorial Atlantic). Stratigraphic ranges of *Petalospyris argiscus* Ehrenberg, 1874; *Petalospyris confluens* Ehrenberg, 1874; *Petalospyris diaboliscus* Ehrenberg, 1847; *Lychnocanium babylonis* (Clark and Campbell, 1942) group; and *Phormocyrtis embolum* (Ehrenberg, 1874) at ODP Site 1260 after Meunier and Danelian (2022). Geomagnetic timescale after calibration of Suganuma and Ogg (2006); and radiolarian biozonations after Meunier and Danelian (2022).

breadth of cephalis 61–70 µm (65), maximum length of lamellar feet 26–64 µm (36).

Remarks.—*Petalospyris castanea* n. sp. differs from most of the other species of the genus *Petalospyris* in having two lateral spines on the cephalis. *Petalospyris castanea* n. sp. resembles *P. diaboliscus* Ehrenberg, 1847, from which it differs in having a latticed thorax, and shorter straight lateral spines on the cephalis. Finally, the new species is distinguished from *P. tricornis* (Haeckel, 1887) in having a thorax shorter than the cephalis height, larger pores, and a smaller number of perioral teeth.

Petalospyris castanea n. sp. appears to have evolved from *P. confluens* in the upper part of the *Podocyrtis* (*L.*) *mitra* Zone, with which it co-occurred afterwards throughout the analyzed stratigraphic interval (Fig. 8). *Petalospyris diaboliscus* evolved from a stock of *P. castanea* n. sp. in the lower part of the *Podocyrtis* (*L.*) *goetheana* Zone. One of the major trends in this evolutionary lineage is the appearance and lengthening of the two lateral horns situated on the cephalis (which developed directly from the latticed shell), the resorption of the thoracic pores, and the lengthening of the perioral teeth. The origin of *P. confluens* remains obscure, and there are no known descendants of *P. diaboliscus*.

Superfamily Archipilioidea Haeckel, 1882, sensu Sandin, Not, and Suzuki in Sandin et al. (2019)
Family Theophormididae Haeckel, 1882, sensu Suzuki emend. Suzuki et al. (2021)
Genus *Velicucullus* Riedel and Campbell, 1952

Type species.—*Soreuma* (*Soreumium*?) *magnificum* Clark and Campbell, 1942, p. 51, pl. 4, fig. 15; by monotypy.

Velicucullus armatus new species
Figure 5.13, 5.14

1973 *Velicucullus* sp. Sanfilippo and Riedel, p. 530, pl. 20, figs. 2, 3 (part).

Holotype.—Figure 5.13; collection number USTL 3277-1; coordinates Q41/1; sample ODP 1260A-14R-5W, 55–57 cm; *Podocyrtis* (*P.*) *ampla* Zone, in the lower part of the *Coccolarnacium periphaenoides* Subzone (late Lutetian, middle Eocene).

Diagnosis.—*Velicucullus* species with four collar pores subequal in size, and a thorax terminating in ~20 well-individualized radial spines.

https://doi.org/10.1017/jpa.2022.82 Published online by Cambridge University Press

Occurrence.—This species occurs sporadically from the *Thyrsocyrtis* (*P.*) *triacantha* Zone, to the upper part of the *Podocyrtis* (*L.*) *mitra* Zone.

Description.—Shell two-segmented, consisting of a large cephalis and a flat extended discoidal thorax. We found no specimens in our material that display an entire cephalis, thus, the anatomical details of the cephalis remain unknown. Basal ring composed of the dorsal spine, the ventral spine, and two primary lateral spines. The four rods intersect orthogonally at angles of 90°, delimiting four collar pores that are subequal in size. Thoracic pores subcircular to quadrangular, roughly aligned longitudinally and increasing in size toward the periphery. Distal margin of the thorax ending in a narrow hyaline band armed with ~20–25 radial spines each spaced by three or four pores and ventrally connected to the velum. Very reduced velum positioned under the most distal row of thoracic pores, not extending on the oral surface of the thorax (Fig. 5.14).

Etymology.—From the Latin *armatus*, meaning 'armed.' The specific epithet is to be treated as an adjective in the nominative singular.

Dimensions.—Based on the only two complete specimens found: shell diameter 251–293 µm.

Remarks.—This species is represented in the fossil record of ODP Site 1260 by highly fragmented remains, including isolated portions of the thorax. However, the very characteristic shape of the distal margin of its thorax does not allow any confusion in its identification, even in the form of small fragments. *Velicucullus armatus* n. sp. differs from *V. discoides* (Ehrenberg, 1874) and *V. fragilis* O'Connor, 1999a, in having the distal margin of the thorax armed with radial spines. The new species differs also from *V. magnificum* (Clark and Campbell, 1942) by having bigger and fewer thoracic pores and well-individualized radial spines, and differs from *V. palaeocenica* in having collar pores equal in size and an almost flat thorax. Finally, *V. armatus* n. sp. co-occurs during its observed stratigraphic range with a gigantic unknown *Velicucullus* species. In our material, this species is always in the form of fragments, and therefore it could not be formally described. In addition to its larger size (>300 µm), this species does not appear to have radial spines, and has smaller and more numerous thoracic pores.

Superfamily Plagiacanthoidea Hertwig, 1879
Family Pseudodictyophimidae Suzuki in Suzuki et al., 2021
Genus *Corythomelissa* Campbell, 1951

Type species.—*Lithomelissa corythium* Ehrenberg, 1874, p. 240 (unfigured); Ehrenberg, 1876, p. 78, pl. 3, fig. 12; subsequent designation by Campbell (1951, p. 529).

Corythomelissa galea (Ehrenberg, 1874) new combination
Figure 4.13–4.16

1874 *Halicalyptra Galea* Ehrenberg, p. 234.
1876 *Halicalyptra Galea*; Ehrenberg, p. 74, pl. 2, fig. 10.
2009 *Halicalyptra galea*; Ogane et al., pl. 44, fig. 2a–g.

Holotype.—No holotype was designated by Ehrenberg in the original description of the species. The specimen drawn by Ehrenberg (1876, pl. 2, fig. 10) and subsequently re-illustrated by Ogane et al. (2009, pl. 44, fig. 2a–g) during their reexamination of Ehrenberg's collection kept in Museum für Naturkunde, Humboldt University (Berlin, Germany), is a candidate lectotype.

Diagnosis.—*Corythomelissa* species with a proportionally small cephalis bearing a strong apical horn and sometimes an inconspicuous ventral horn, a closed thorax, and three straight, downwardly directed feet.

Occurrence.—*Corythomelissa galea* (Ehrenberg, 1874) n. comb. has a discontinuous range at ODP Site 1260, extending from the upper part of the *Podocyrtis* (*P.*) *ampla* Zone, to the lower part of the *Podocyrtis* (*L.*) *mitra* Zone.

Description.—Shell composed of two segments, globular, and thick-walled. Cephalis subspherical to hemispherical, partially embedded in the thorax, and penetrated by randomly distributed subcircular pores. Apical spine free in the cephalic cavity and extending outside as a stout, bladed apical horn. Ventral spine protruding as a small sagittal horn in some specimens (Fig. 4.16). Dorsal and primary lateral spines elongated as strong ribs or ridges on the thorax, and protruding as three straight bladed feet. Thorax usually closed distally, rounded and asymmetrical in lateral view due to development of the dorsal spine. Thoracic pores subcircular to elongated around the thoracic ribs, irregular in size, generally larger than cephalic ones.

Dimensions.—Based on five specimens (mean): length of cephalothorax without the apical horn 82–105 µm (90), length of apical horn 21–35 µm (29), length of feet 53–86 µm (64).

Remarks.—*Corythomelissa galea* (Ehrenberg, 1874) n. comb. was assigned to the genus *Corythomelissa* on the basis of its closed thorax, its hemispherical cephalis bearing an apical and a ventral spine, and its dorsal and primary lateral spines prolonged as three straight, downwardly directed feet. The combination *Phaenocalpis galea* (Ehrenberg, 1874), recently suggested by O'Dogherty et al. (2021), was not selected because the species belonging to the genus *Phaenocalpis* are all composed of a single segment. *Corythomelissa galea* (Ehrenberg, 1874) n. comb differs from *C. horrida* (Petrushevskaya, 1975) group, *C. omoprominentia* Funakawa, 1995a, and *C. spinosa* Funakawa, 1995a, in having a smooth-surfaced cephalis bearing shorter apical and ventral horns, and differs from *C. pachyostraca* Funakawa, 1995a, in having a smaller cephalis with shorter apical and ventral horns, and a closed thorax. Among similar-looking *Pseudodictyophimus* species, *C. galea* (Ehrenberg, 1874) n. comb. differs from *Ps. bicornis* (Ehrenberg, 1874), *Ps. leptoretis* Funakawa, 1995b, *Ps. pyramidalis* Funakawa, 1995b, and *Ps. tanythorax* Funakawa, 1994, in having a shorter ventral horn, three straight, downwardly directed feet,

https://doi.org/10.1017/jpa.2022.82 Published online by Cambridge University Press

and a closed thorax. It is also distinguished from *Ps.*? *sphaerothorax* Funakawa, 1995b, in having a smaller ventral horn and a proportionally larger thorax, and from *Ps.*? *charlestonensis* (Clark and Campbell, 1945) in having three straight feet, and a cephalis conspicuously embedded in the thorax. Finally, *C. galea* (Ehrenberg, 1874) n. comb. differs from *Spongomelissa cucumella* Sanfilippo and Riedel, 1973, in having larger pores, a cephalis distinctly smaller than the thorax, and three longer feet.

Superfamily Lithochytridoidea Ehrenberg, 1846
Family Lithochytrididae Ehrenberg, 1846, sensu Suzuki in Matsuzaki et al. (2015)
Genus *Lychnocanium* Ehrenberg, 1846

Type species.—*Lychnocanium lucerna* Ehrenberg, 1847, p. 55, fig. 5; subsequent monotypy (O'Dogherty et al., 2021).

Lychnocanium nimrodi new species
Figure 5.9–5.12

1985 *Sethochytris babylonis* group; Sanfilippo et al., fig. 17.8a (part).

Holotype.—Figure 5.9; collection number USTL 3483-2; coordinates L38/2; sample ODP 1260A-9R-4W, 55–57 cm; upper part of the *Podocyrtis* (*L.*) *mitra* Zone, in the *Podocyrtis* (*P.*) *apeza* Subzone (late Lutetian, middle Eocene).

Diagnosis.—*Lychnocanium* species with a stout, distally dilated apical horn, and three long subparallel feet, rectangular in cross-section.

Occurrence.—*Lychnocanium nimrodi* n. sp. ranges from the upper part of the *Podocyrtis* (*L.*) *mitra* Zone to the lowermost part of the *Podocyrtis* (*L.*) *chalara* Zone.

Description.—Cephalis subspherical, thick-walled, and poreless. Apical horn longer than the cephalis, stout and distally dilated, with a hammered surface. Collar stricture well defined externally by a change in the shell contour. Thorax pyriform, with subcircular pores of different sizes, quincuncially or irregularly arranged. Three long and subparallel feet, rectangular in cross section and dilated at the end in heavily silicified specimens (Figs. 5.9, 5.11), emerging from the base of the thorax. Feet smooth-surfaced over a large part of their length, then rough-surfaced when they are dilated.

Etymology.—Named after Nimrod, the ancient king of Babylon who commissioned the construction of the Tower of Babel. The specific epithet is to be treated as a noun in the genitive case formed from a personal name.

Dimensions.—Based on 20 specimens (mean): length of cephalothorax without the apical horn 81–107 µm (91), length of apical horn 35–59 µm (46), length of feet 88–140 µm (117).

Remarks.—*Lychnocanium nimrodi* n. sp. is undoubtedly related to the *L. babylonis* (Clark and Campbell, 1942) group. It is distinguished from all morphotypes grouped under this name in having a rounded thorax rather than a pyramidal thorax with sharp angles, and in having three long subparallel feet, rectangular in cross section and usually distally dilated. A distally dilated apical horn is also a characteristic feature of *L. nimrodi* n. sp.

This short-lived species is regarded as an offshoot from the *L. babylonis* group (Fig. 8).

Superfamily Pterocorythoidea Haeckel, 1882, emend. Suzuki et al. (2021)
Family Lophocyrtiidae Sanfilippo and Caulet in De Wever et al., 2001
Genus *Aphetocyrtis* Sanfilippo and Caulet, 1998

Type species.—*Aphetocyrtis gnomabax* Sanfilippo and Caulet, 1998, p. 16, pl. 7, fig. 10.

Aphetocyrtis zamenhofi new species
Figure 6.1–6.4, 6.8

2006 *Lophocyrtis* (*Apoplanius*) *aspera* (Ehrenberg); Funakawa et al., p. 25, pl. P7, figs. 5a, b (part).

Holotype.—Figure 6.1; collection number USTL 3543-1; coordinates Q37/4; sample 1260A-15R-2W, 55–57 cm; lowermost part of the *Podocyrtis* (*P.*) *ampla* Zone, in the *Dictyomitra amygdala* Subzone (late Lutetian, middle Eocene).

Diagnosis.—*Aphetocyrtis* species with an apical spine completely free in the cephalic cavity, an inflated hemispherical thorax, and an abdomen split in half by constriction.

Occurrence.—From the beginning of the studied interval, which is situated in the *Thyrsocyrtis* (*P.*) *triacantha* Zone, to the upper part of the *Podocyrtis* (*P.*) *ampla* Zone.

Description.—Three-segmented, thick-walled, and almost cylindrical shell. Cephalis proportionally small, spherical and globular, porous. Apical spine merge with the cephalic wall, protruding outside as a small simple apical horn. Collar constriction expressed externally by a sharp contour change that gives the impression that the cephalis is just resting on the thorax. Thorax inflated hemispherically, perforated by subcircular pores that are regular in size and shape, quincuncially arranged, and hexagonally framed by high and sharp ridges that give the thorax its thorny contour. Lumbar stricture marked by a thick internal ridge, which appears externally as an obscure band. Abdomen in the form of an hourglass, with an inflated proximal part followed by a constriction and then an enlargement of the shell. Abdominal pores subcircular to ovoid, unequal in size, randomly distributed or roughly aligned longitudinally. In the proximal part of the abdomen, pores separated by weak ridges, sometimes fused and arranged longitudinally according to the alignment of the pores. Abdominal termination lacks a peristome or terminal feet.

Etymology.—Named after the Polish ophthalmologist Ludwik Lejzer Zamenhof, who is the creator of Esperanto, one of the

https://doi.org/10.1017/jpa.2022.82 Published online by Cambridge University Press

most widely used constructed international auxiliary languages. The specific epithet is to be treated as a noun in the genitive case formed from a modern personal name.

Dimensions.—Based on 30 specimens (mean): total length 120–258 μm (188), length of cephalothorax 61–107 μm (84), length of abdomen 59–157 μm (104).

Remarks.—*Aphetocyrtis zamenhofi* n. sp. displays strong morphological similarities to early representatives of *A. gnomabax* Sanfilippo and Caulet, 1998, which can have a constricted abdomen (e.g., Sanfilippo and Caulet, 1998, pl. 2, figs. 14–17). However, *A. zamenhofi* n. sp. is distinguished from *A. gnomabax* by having an apical spine completely free in the cephalic cavity, a more globular cephalis that is well separated from the thorax, and an inflated hemispherical thorax rather than an inflated campanulate thorax. In addition to the organization of its initial spicule, *A. zamenhofi* n. sp. differs from the Southern Ocean species *A. rossi* Sanfilippo and Caulet, 1998, and *A. catalexis* Sanfilippo and Caulet, 1998, and from the tropical species *A.*? *columboi* n. sp. in having a constricted abdomen. The new species is separated from *A.*? *bianulus* (O'Connor, 1997b) by its shorter abdomen with only one constriction. During a part of its range, *A. zamenhofi* n. sp. co-occurs with *Lophocyrtis alauda* (Ehrenberg, 1874), which is easy to differentiate by its stronger apical horn and its subcylindrical abdomen perforated by pores that are regular in size and shape. Among the lophocyrtiids, *Apoplanius klydus* (Sanfilippo and Caulet, 1998) also has an undulating abdomen, but differs from *A. zamenhofi* n. sp. in having a spiny thorax, an apical spine partially included within the cephalis wall, and a stronger apical horn.

Under the original description of the genus *Aphetocyrtis*, Sanfilippo and Caulet (1998) described three species (*A. gnomabax*, *A. rossi*, and *A. catalexis*), all of which were included in the *A. gnomabax* lineage. One of the major trends in this evolutionary lineage during the late Paleogene is the gradual inclusion of the apical spine in the cephalic wall. In *A. gnomabax*, the earliest morphospecies of this lineage, known during the earliest middle Eocene, the apical spine is loosely attached to the cephalic wall; the apical spine becomes completely included in the cephalic wall in the youngest Oligocene morphospecies *A. rossi* and *A. catalexis*. The apical spine of *A. zamenhofi* n. sp., which is completely merged in the cephalic wall (Fig. 6.8), prevents inclusion of this species in the *A. gnomabax* lineage. Therefore, *A. zamenhofi* n. sp. is not considered as a descendant of *A. gnomabax*, in spite of their great morphological similarity; it is likely part of another evolutionary lineage within the genus *Aphetocyrtis*. Documentation of *A. zamenhofi* n. sp. allows firm placement of the origin of the genus *Aphetocyrtis* in low latitudes in the middle Eocene, before its migration to high latitudes during the late Eocene (Sanfilippo and Caulet, 1998).

Aphetocyrtis? *columboi* new species
Figure 6.5–6.7, 6.9

Holotype.—Figure 6.5; collection number USTL 3438-1; coordinates J31/1; sample ODP 1260A-6R-6W, 55–57 cm; lowermost part of the *Podocyrtis* (*L.*) *goetheana* Zone (early Bartonian, middle Eocene).

Diagnosis.—Spindle-shaped shell with a tapered abdomen, terminating in a horn-like structure.

Occurrence.—From the upper part of the *Podocyrtis* (*L.*) *chalara* Zone to the *Podocyrtis* (*L.*) *goetheana* Zone.

Description.—Shell three-segmented, spindle-shaped, and thick-walled, with the collar and lumbar strictures expressed externally as a slight contour change. Cephalis spheroidal to flattened ovoid, partially embedded in the thorax, poreless or with a few small and irregularly distributed pores. Apical spine included in the cephalic wall, protruding externally as a reduced apical horn, shorter than the cephalis height. Mitral arches leave the apical spine in the middle of the cephalis, and diverge rapidly at a great angle. Thorax hemispherical to inflated campanulate, as wide as, or wider than, the abdomen, with subcircular pores quincuncially arranged. Dorsal and primary lateral spines prolonged in the thoracic wall as externally indistinct ribs, protruding outside the shell as three inconspicuous conical wings that usually are broken and difficult to see (Fig. 6.5). Abdomen inverted conical, with subcircular pores roughly arranged in longitudinal rows. Abdomen terminating in a horn-like structure, usually longer than the apical horn (Fig. 6.5), but ragged along a pore row in most of the observed specimens (Fig. 6.6, 6.7).

Etymology.—Named after the iconic cigar smoker Lieutenant Columbo of the eponym American crime drama series Columbo, for the resemblance of this species to a cigar. The specific epithet is to be treated as a noun in the genitive case formed from a modern personal name.

Dimensions.—Based on 11 specimens (mean): total length 191–207 μm (193), length of cephalothorax 71–84 μm (77), length of abdomen 101–121 μm (116).

Remarks.—*Aphetocyrtis*? *columboi* n. sp. is tentatively assigned to the genus *Aphetocyrtis* because of the general morphology of its shell and the organization of its initial spicule. Its phylogenetic relationships with other members of the *A. gnomabax* lineage are difficult to determine for now; however, it can be noted that this new species has reached an advanced stage in the inclusion of the apical spine in the cephalic wall early in the history of the genus (Fig. 6.9). *Aphetocyrtis*? *columboi* n. sp. is distinguished from *A. gnomabax* Sanfilippo and Caulet, 1998, *A. rossi* Sanfilippo and Caulet, 1998, *A. catalexis* Sanfilippo and Caulet, 1998, and *A. zamenhofi* n. sp. by its tapered abdomen terminating in a horn-like structure and its thorax flanked by three small wings. This new species is morphologically close to *A.*? *hamata* (O'Connor, 1999a), from which it differs in being larger and in having more regularly arranged abdominal pores. *Aphetocyrtis*? *columboi* n. sp. is also distinguished from *Lophocyrtis versipellis* (Ehrenberg, 1874) by having a flattened ovoid cephalis and smaller abdominal pores. In general form, *A.*? *columboi* n. sp. is superficially similar to some species of the genus *Glomaria*, in particular the middle Miocene

https://doi.org/10.1017/jpa.2022.82 Published online by Cambridge University Press

species *G. thornburgi* (Sanfilippo and Riedel, 1970) and *G. baueri* (Sanfilippo and Riedel, 1970). However, the thorax of *A.*? *columboi* n. sp. is not composed of a loose spongy meshwork, which differentiates it easily from all the species of the genus *Glomaria*.

The origin of *A.*? *columboi* n. sp. remains obscure; it is probably closely related to the late Eocene species *A.*? *hamata* (O'Connor, 1999a), which was described from the Oamaru Diatomite.

Aphetocyrtis? *spheniscus* new species
Figure 6.10–6.13

Holotype.—Figure 6.10; collection number USTL 2851-2; coordinates Y49/1; sample ODP 1260A-12R-1W, 55–57 cm; lower part of the *Podocyrtis* (*L.*) *mitra* Zone, in the *Artostrobus quadriporus* Subzone (late Lutetian, middle Eocene).

Diagnosis.—*Aphetocyrtis* species with an elongated shell, a slight abdominal constriction, and an open aperture.

Occurrence.—From the lowermost part of the *Podocyrtis* (*P.*) *ampla* Zone, to the lower part of the *Podocyrtis* (*L.*) *chalara* Zone.

Description.—Shell of three segments, subcylindrical to fusiform, and thick-walled. Cephalis subspherical, perforated by few subcircular pores and bearing a strong bladed apical horn. Collar stricture expressed as a change in the shell contour. Thorax thick-walled, campanulate to truncated-conical, with circular pores quincuncially arranged. Thoracic stricture marked externally by a slight constriction of the shell, and lined by an internal ridge that appears externally as an obscure band. The pores on the thoracic stricture are slightly lengthened longitudinally. Abdomen subcylindrical, with circular pores longitudinally aligned, although pore alignment tends to be less regular in the distal part of the abdomen. Short longitudinal ridges sometimes separate rows of abdominal pores (Fig. 6.11). Aperture sometimes slightly constricted, and always ragged.

Etymology.—From the Latin *spheniscus*, meaning 'penguin,' for its resemblance to the great penguins. The specific epithet is to be treated as a noun in the nominative singular standing in apposition to the generic name.

Dimensions.—Based on 30 specimens (mean): total length 130–214 µm (159), length of apical horn 12–23 µm (15), length of cephalothorax 70–102 µm (80), length of abdomen 62–144 µm (80).

Remarks.—*Aphetocyrtis*? *spheniscus* n. sp. is tentatively assigned to the genus *Aphetocyrtis* because of the absence of a ventral horn or of any external extensions related to the dorsal and the primary lateral spines, and because of its abdomen ending in a simple peristome. The new species is morphologically close to the specimen designated as holotype of the species *A. catalexis* Sanfilippo and Caulet, 1998 (pl. 7, fig. 14a, b), but it differs in having a truncate conical thorax rather than a hemispherical thorax, and less-marked abdominal and collar constrictions. *Aphetocyrtis*? *spheniscus* n. sp. also differs from *A. saginata* (Takemura and Ling, 1998) in having smaller thoracic and abdominal pores, as well as a less-pronounced constriction between the thorax and the abdomen. It differs from *A. minuta* (Takemura and Ling, 1998) and *A. perforalvus* (O'Connor, 1997b) in being more elongated, with a truncate conical thorax rather than an hemispherical to spherical thorax, and in having a stronger apical horn, and from *A. spongoconus* (Kling, 1971) in having a latticed abdomen instead of a spongious abdomen. *Aphetocyrtis*? *spheniscus* n. sp. is also distinguished from *Theocyrtis diabloensis* Clark and Campbell, 1942, and *T. robusta* Clark and Campbell, 1942, in having a less-pronounced lumbar stricture and regularly arranged pores, and from *T. kerguelensis* Takemura and Ling, 1998, in having a shorter apical horn, and regular abdominal pores in size and shape. Finally, *A.*? *spheniscus* n. sp. can be distinguished from *Paralampterium*? *robusta* (Clark and Campbell, 1942) by its less-pronounced lumbar structure and its shorter apical horn, and from *P.*? *scolopax* (Ehrenberg, 1874) by its shorter apical horn, its smaller thoracic and abdominal pores, and by the absence of well-differentiated longitudinal ridges separating the rows of abdominal pores.

Family *Pterocorythidae* Haeckel, 1882
Genus *Albatrossidium* Sanfilippo and Riedel, 1992

Type species.—*Albatrossidium minzok* Sanfilippo and Riedel, 1992, p. 16, pl. 2, fig. 7.

Albatrossidium regis new species
Figure 6.14–6.17

Holotype.—Figure 6.14; collection number USTL 2851-1; coordinates Y54/2; sample 1260A-12R-1W, 55–57 cm; lower part of the *Podocyrtis* (*L.*) *mitra* Zone, in the *Artostrobus quadriporus* Subzone (late Lutetian, middle Eocene).

Diagnosis.—*Albatrossidium* species with a cylindrical shell, a large triangular apical horn, and spaced, irregularly arranged pores in the distal part of the abdomen.

Occurrence.—From the beginning of the studied interval, which is situated in the *Thyrsocyrtis* (*P.*) *triacantha* Zone, to the upper part of the *Podocyrtis* (*L.*) *mitra* Zone.

Description.—Three-segmented, cylindrical, and thick-walled shell. Cephalis hemispherical and trilobate, bearing a strong pyramidal apical horn and sometimes a few small accessory spines on the rim of the cephalic hole. Cephalic pores subcircular, few in number, and randomly arranged. Inconspicuous collar stricture. Thorax subcylindrical to campanulate, with subcircular pores hexagonally framed and quincuncially arranged. The boundary between thorax and abdomen is marked by an internal ring, which appears externally as an obscure band. Abdomen cylindrical, with subcircular pores longitudinally aligned in the proximal part, then smaller, irregularly arranged, and more spaced. Abdomen terminating in an simple, almost hyaline peristome, or in three inconspicuous shovel-shaped feet.

https://doi.org/10.1017/jpa.2022.82 Published online by Cambridge University Press

Etymology.—This species is named after the late radiolarian specialist Dr. William Rex Riedel, who actively participated in the renewal of radiolarian studies during the second part of the twentieth century. The specific epithet is to be treated as a noun in the genitive case formed from a personal name that is Latin.

Dimensions.—Based on 14 specimens (mean): total length without the apical horn 76–167 µm (121), length of apical horn 26–38 µm (31), length of cephalothorax without the apical horn 62–93 µm (70), length of abdomen 39–85 µm (55).

Remarks.—*Albatrossidium regis* n. sp. is distinguished from the holotype of *A. minzok* (Sanfilippo and Riedel, 1992, pl. 2, fig. 7) in having a large triangular apical horn and three shovel-shaped feet. The new species differs from *A. cylindricum* (Ehrenberg, 1874) and *A. tenellum* (Foreman, 1973) in having a more elongated apical horn, usually flanked by a few accessory spines close to its base, and by the proportion of thoracic length to abdominal length: 1:1 to 1:1.5 in the former, while it is greater than 1:2 for the other two species mentioned. Finally, *A. regis* n. sp. differs from *A. annikasanfilippoae* n. sp. in being much more cylindrical, with a reduction in the number of pores in the distal part of the abdomen, in having smaller accessory spines, and in not having any perforation in the apical horn.

Albatrossidium minzok is considered to be the ancestral species of the genus (Sanfilippo and Riedel, 1992). Given its stratigraphic position (early Eocene to middle Eocene), this species represents a potential ancestor for the late middle Eocene species *A. regis* n. sp. However, the phylogenetic relationship between these two species could not be elucidated in this study due to the absence of *A. minzok* at ODP Site 1260. A few specimens with a large triangular apical horn and a long cylindrical abdomen perforated by regularly arranged pores were observed in the *Podocyrtis* (*L.*) *goetheana* Zone after the last occurrence of *A. regis* n. sp. These specimens correspond well to *A. cylindricum* as described by Ehrenberg (1874, p. 227) and illustrated by Ogane et al. (2009, pl. 84, figs. 5a–d, pl. 85, figs. 1a–d). Given their morphological resemblance to *A. regis* n. sp. and their stratigraphic position, these specimens may represent the descendants of *A. regis* n. sp.

Albatrossidium annikasanfilippoae new species
Figure 7.1–7.4

1992 *Albatrossidium minzok* Sanfilippo and Riedel, p. 18, pl. 1, fig. 18 (part).

Holotype.—Figure 7.1; collection number USTL 3512-1; coordinates Y39/1; sample ODP 1260A-12R-3W, 55–57 cm; lower part of the *Podocyrtis* (*L.*) *mitra* Zone, in the *Artostrobus quadriporus* Subzone (late Lutetian, middle Eocene).

Diagnosis.—*Albatrossidium* species with a large triangular and perforated apical horn, surrounded by several accessory spines.

Occurrence.—From the lower part of the *Podocyrtis* (*P.*) *ampla* Zone, to the end of the studied interval, which is situated in the lower part of the *Podocyrtis* (*L.*) *goetheana* Zone.

Description.—Three-segmented, smooth, and thick-walled shell. Cephalis trilobate, hemispherical, bearing a strong triangular apical horn and usually two or four accessory spines on the rim of the cephalic hole. Proximal half of the apical horn usually perforated by several subcircular pores. Cephalic pores subcircular and randomly arranged. Collar stricture expressed externally as a slight contour change. Thorax campanulate to inflated campanulate, with quincuncially arranged subcircular pores with polygonal pore-frames. Thorax and abdomen separated by an internal septa that is marked externally by a slight change in the shell contour. Abdomen subcylindrical, with subcircular pores roughly arranged in longitudinal rows. Abdominal termination undifferentiated, invariably ragged along a pore row.

Etymology.—The species is dedicated to Dr. Annika Sanfilippo for her cornerstone work on Paleogene radiolarians. The specific epithet is to be treated as a noun in the genitive case formed from a modern personal name.

Dimensions.—Based on 26 specimens (mean): total length without the apical horn 110–174 µm (126), length of apical horn 30–47 µm (39), length of cephalothorax without the apical horn 61–100 µm (77), length of abdomen 29–87 µm (49).

Remarks.—*Albatrossidium annikasanfilippoae* n. sp. differs from the holotype of *A. minzok* (Sanfilippo and Riedel, 1992, pl. 2, fig. 7), *A. cylindricum* (Ehrenberg, 1874), and *A. tenellum* (Foreman, 1973) in having a perforated apical horn surrounded by several accessory spines, and an abdomen shorter than the thorax. *Albatrossidium annikasanfilippoae* n. sp. differs from *A. regis* n. sp. as reported under *A. regis* n. sp.

Given that *A. minzok* is the earliest member of the genus *Albatrossidium*, known from the early Eocene to the middle Eocene (Sanfilippo and Riedel, 1992), it seems to be a possible ancestor of the late middle Eocene species *A. annikasanfilippoae* n. sp. However, *A. minzok* was not found at ODP Site 1260, and for this reason it is for the moment impossible to confirm this phylogenetic hypothesis. The cephalic hole observed in *A. annikasanfilippoae* n. sp. reminds us the open cephalis of Neogene and Quaternary species of the genus *Lamprocyrtis* (e.g., Sanfilippo and Riedel, 1992, pl. 4, figs. 7–9). However, the rest of the cephalis of *Lamprocyrtis* species differs in being longitudinally elongated and indistinctly trilobed. Although the two genera are related (Sanfilippo and Riedel, 1992), it is likely that this remarkable cephalic structure appeared twice independently.

Genus *Phormocyrtis* Haeckel, 1887

Type species.—*Phormocyrtis longicornis* Haeckel, 1887, p. 1370, pl. 69, fig. 15; subsequent designation by Campbell (1954, p. D134).

https://doi.org/10.1017/jpa.2022.82 Published online by Cambridge University Press

Phormocyrtis lazari new species
Figure 7.5–7.8

1957 *Phormocyrtis embolum*; Riedel, p. 88, pl. 2, fig. 7 (part).
1972 *Phormocyrtis embolum* group; Petrushevskaya and Kozlova, p. 537, pl. 22, figs. 8, 9.
1974 *Phormocyrtis embolum*; Kruglikova, fig. 3.10.
1975 *Phormocyrtis proxima* (?); Chen, p. 456, pl. 2, fig. 6.
?1999 *Phormocyrtis embolum*; Kozlova, p. 148, pl. 31, fig. 14.
?1999 *Phormocyrtis* sp. cf. *P. embolum*; Kozlova, pl. 35, fig. 16.

Holotype.—Figure 7.5; collection number USTL 3474-1; coordinates T40/4; sample 1260A-9R-2W, 55–57 cm; uppermost part of the *Podocyrtis* (*L.*) *mitra* Zone, in the *Podocyrtis* (*P.*) *apeza* Subzone (late Lutetian, Middle Eocene).

Diagnosis.—*Phormocyrtis* species with a subcylindrical hyaline abdomen terminated by lamellar feet.

Occurrence.—From the upper part of the *Podocyrtis* (*L.*) *mitra* Zone, to the end of the studied interval, which is situated in the lower part of the *Podocyrtis* (*L.*) *goetheana* Zone.

Description.—Shell three-segmented, smooth, and thick-walled, with the collar and lumbar strictures slightly expressed externally. Cephalis hemispherical, poreless or with a few small subcircular pores, bearing short conical horn, weakly bladed, at least in the proximal part. Thorax truncate conical to subcylindrical, with pores in longitudinal rows (6–7 in a row), separated by strong longitudinal ribs. The lower margin of the thorax marked by a well-defined internal septal band. Abdomen subcylindrical to truncate conical, hyaline or sparsely pored in its upper portion, then surrounded by ~20 lamellar feet pointing distally and variable in length (~0.5–2 times the length of the hyaline part). Abdominal pores, when present, subcircular or longitudinally elongated, and can be up to three times as long as the thoracic pores.

Etymology.—This species is named in honor of Dr. David Lazarus (Museum für Naturkunde, Humboldt-Universität, Berlin) for his contribution to the study of Cenozoic radiolarians. The specific epithet is to be treated as a noun in the genitive case formed from a personal name that is Latin.

Dimensions.—Based on 30 specimens (mean): total length without the apical horn 69–180 µm (129), length of apical horn (when present) 7–15 µm (12), length of cephalothorax without the apical horn 51–84 µm (72), length of the hyaline proximal part of the abdomen 18–40 µm (27), length of lamellar feet 6–68 µm (33).

Remarks.—*Phormocyrtis lazari* n. sp. differs from *P. embolum* (Ehrenberg, 1874), *P. ligulata* Clark and Campbell, 1942, and *P. striata* Brandt, 1935, by having a subcylindrical, sparsely pored abdomen terminated by lamellar feet, rather than an inverted truncate conical abdomen with numerous pores and a simple peristome. *Phormocyrtis lazari* n. sp. also differs from all *P. striata* subspecies by the presence of an internal septal band at the lower margin of the thorax. *Phormocyrtis lazari* n. sp. is distinguished from *P. proxima* Clark and Campbell, 1942, by having a nearly hyaline abdomen terminated by lamellar feet, and from *P. alexandrae* O'Connor, 1997a, *P.*? *cubense* Riedel and Sanfilippo, 1971, and *P. turgida* (Krasheninnikov, 1960) in having no fourth segment.

Stratigraphic data collected at ODP Site 1260 suggest that *P. lazari* n. sp. is derived from *P. embolum*; the latter species disappeared shortly after the first occurrence of *P. lazari* n. sp. (Fig. 8). The two species share many morphological similarities: towards the end of its age range, *P. embolum* tends to become more cylindrical, with a subcylindrical to slightly tapered abdomen. This late morphotype of *P. embolum* corresponds well to the original description of *P. proxima*, and argues for the synonymization of these two species. Riedel (1957) had already suggested this, and extended it to specimens bearing an abdomen terminated by lamellar teeth, although the original description of *P. proxima* does not mention the presence of such perioral appendages. A few specimens exhibiting an intermediate morphology between *P. embolum* and *P. lazari* n. sp. also have been observed at ODP Site 1260, as well as in the Southern Ocean (Hollis et al., 2020, pl. 10, fig. 18). These specimens are characterized by a subcylindrical porous abdomen terminated by short lamellar teeth. *Phormocyrtis ligulata* is also probably related to these taxa. Unfortunately, this species was only reported from the Pacific Ocean (Clark and Campbell, 1942, 1945; Blueford, 1988) and from the Southern Ocean (O'Connor, 1999b; Hollis et al., 2020), therefore we were unable to clarify its phylogenetic relationships with *P. embolum* and *P. lazari* n. sp.

Genus *Podocyrtis* Ehrenberg, 1846

Type species.—*Podocyrtis papalis* Ehrenberg, 1847, p. 55, fig. 2; subsequent designation Campbell (1954, p. D130).

Podocyrtis (Lampterium) puellasinensis Ehrenberg, 1874
Figure 7.9–7.11

1874 *Podocyrtis Puella sinensis* Ehrenberg, p. 252.
1876 *Podocyrtis Puella sinensis*; Ehrenberg, p. 82, pl. 14, fig. 3.
2009 *Podocyrtis puella-sinensis*; Ogane et al., pl. 48, figs. 9a–f.

Holotype.—No holotype was designated by Ehrenberg (1874) in the original description of the species. The specimen drawn by Ehrenberg (1876, pl. 14, fig. 3) and subsequently re-illustrated by Ogane et al. (2009, pl. 48, fig. 9a–f) during their reexamination of Ehrenberg's collection kept in Museum für Naturkunde, Humboldt University (Berlin, Germany), is a candidate lectotype.

Diagnosis.—*Podocyrtis* species with a two-segmented shell, and a well-defined cephalic hole delimited by a thick hyaline rim.

Occurrence.—From the upper part of the *Podocyrtis* (*P.*) *ampla* Zone, to the end of the studied interval, which is situated in the lower part of the *Podocyrtis* (*L.*) *goetheana* Zone.

https://doi.org/10.1017/jpa.2022.82 Published online by Cambridge University Press

Description.—Shell two-segmented and robust. Cephalis trilobed, with one large unpaired eucephalic lobe, and two small paired lobes dorsally positioned. Cephalic pores subcircular to quadrate, irregular in size, and randomly arranged. Apical horn long as the cephalis, triangular, with a large cephalic hole circumscribed by a thick hyaline rim. Thorax truncate conical to globular, perforated by subcircular pores of various size, usually hexagonally framed, and much larger than the cephalic ones. Thorax ending in a smooth hyaline peristome doubled by an internal septum, or more rarely ending in a crown of very short spines (Fig. 7.11).

Dimensions.—Based on 18 specimens (mean): length of cephalothorax without the apical horn 65–90 µm (78), length of the apical horn 27–51 µm (41), maximum breadth of shell 66–92 µm (78).

Remarks.—*Podocyrtis* (*L.*) *puellasinensis* Ehrenberg, 1874 is distinguished from all other *Podocyrtis* species by its two-segmented shell and its well-developed cephalic hole.

We have chosen to leave *P.* (*L.*) *puellasinensis* in the genus *Podocyrtis*, although the absence of an abdominal segment in this species is in contradiction with the diagnosis of the genus (O'Dogherty et al., 2021). This choice was motivated by the strong morphological similarities between *P.* (*L.*) *puellasinensis* and the cephalothorax of the later members of the subgenus *Lampterium*, such as *P.* (*L.*) *chalara* Riedel and Sanfilippo, 1970, and *P.* (*L.*) *goetheana* (Haeckel, 1887) (see Fig. 7.12 for comparison with a typical *P.* [*Lampterium*] cephalothorax). This resemblance is all the more unexpected because the first occurrence of *P.* (*L.*) *puellasinensis* is dated 43.36 Ma at ODP Site 1260, ca. 2.2 Ma earlier than the first occurrence of *P.* (*L.*) *chalara* (41.15 Ma; Meunier and Danelian, 2022). It is therefore difficult to decipher the origin of *P.* (*L.*) *puellasinensis*. The best candidate seems to be *P.* (*L.*) *sinuosa* Ehrenberg, 1874, although its thorax is more campanulate and penetrated by smaller pores. In this case, *P.* (*L.*) *puellasinensis* would be an offshoot of the lineage from *P.* (*L.*) *sinuosa* to *P.* (*L.*) *mitra*, and for this reason it is placed in the subgenus *Lampterium*. In their taxonomic review, O'Dogherty et al. (2021) recognized the subgenus *Lampterium* as a distinct genus, and suggested the following combinations: *Lampterium chalara* (Riedel and Sanfilippo, 1970) and *L. goetheana* (Haeckel, 1887). We do not share this view because the *Lampterium* evolutionary lineage that leads from *P.* (*L.*) *acalles* Sanfilippo and Riedel, 1992, to *P.* (*L.*) *goetheana* has been amply demonstrated (e.g., Riedel and Sanfilippo, 1970; Sanfilippo and Riedel, 1992), and this taxonomic change would imply that the genus *Podocyrtis* is paraphyletic. An alternative hypothesis to explain the particular morphology of *P.* (*L.*) *puellasinensis* is that this species is the expression of an early stage in the development of the *Podocyrtis* shell (a neoteny).

Conclusions

Examination of middle Eocene sediment sequences from the equatorial Atlantic Ocean allowed the description of 15 new radiolarian species, and the re-illustration of four species rarely reported since their original description in early radiolarian studies. With the exception of a few sporadic species (*Petalospyris castanea* n. sp., *Pterocyrtidium eep* n. sp., *Cymaetron*? *dilatatus* n. sp., and *Velicucullus armatus* n. sp.), the taxa reported herein have a continuous range in the studied interval, and can therefore be included in future biostratigraphic studies. Although the studied interval is relatively limited and did not allow us to establish the total range of most of these species, 23 radiolarian bioevents are documented, including 14 first occurrences and nine last occurrences. Orbitally tuned ages are provided for these bioevents through direct calibration to the astronomical time scale, increasing the number of biostratigraphic tiepoints available for the equatorial Atlantic Ocean.

Several new species described herein display strong morphological similarities to previously described species, which enabled us to suggest phylogenetic hypotheses by integrating stratigraphic data. Despite being fragmentary, these observations are important in establishing new evolutionary lineages, and better understand nassellarian evolutionary dynamics. The documentation of new species has also improved our understanding of the origin of some genera. This is the case of the genus *Aphetocyrtis*, which is now clearly rooted in the tropical region with three new tropical species reported herein (*A. zamenhofi* n. sp., *A.*? *columboi* n. sp., and *A.*? *spheniscus* n. sp.). Similarly, documentation of *Spirocyrtis*? *renaudiei* n. sp., an Artostrobiid species with a mixture of characters found in the genera *Botryostrobus* and *Spirocyrtis*, allows us to place the divergence between these two genera shortly before the late middle Eocene. Finally, this study contributed to the addition of new species to the monotypic genera *Albatrossidium* and *Cymaetron*, which are poorly known and have been rarely reported since their original descriptions.

Acknowledgments

We thank the Ocean Drilling Program (ODP) for supplying the samples used in this study. Thanks also to J. Cuvelier for technical assistance. Constructive remarks by the two anonymous reviewers significantly improved the initial manuscript.

Declaration of competing interests

The authors declare none.

Data availability statement

Biostratigraphic data generated in this study are available in Supplementary Data 1, reposited in the Dryad Digital Repository: https://doi.org/10.5061/dryad.x3ffbg7nn.

References

Bailey, J.W., 1856, Notice of microscopic forms found in the soundings of the Sea of Kamtschatka—with a plate: American Journal of Science and Arts, ser. 2, v. 22, p. 1–6.

Blueford, J., 1988, Radiolarian biostratigraphy of siliceous Eocene deposits in central California: Micropaleontology, v. 34, p. 236–258.

Brandt, R., 1935, Radiolaria, *in* Wetzel, O., ed., Die Mikropalaontologie des Heiligengener Kieseotones (Ober-Eozän). Siebenundzwanzigster Jahresbericht des Niedersächsischen geologischen Vereins: Geologische Abteilung der Naturhistorischen Gesellschaft zu Hannover, v. 27, p. 41–81.

https://doi.org/10.1017/jpa.2022.82 Published online by Cambridge University Press

Bury, P.S., 1862, Polycystins, Figures of Remarkable Forms & c., in the Barbados Chalk Deposit, (Chiefly Collected by Dr. Davy, and Notice in a Lecture to the Agricultural Society of Barbados, in July, 1846): London, W. Weldon, 8 p.

Bütschli, O., 1882a, Beiträge zur Kenntnis der Radiolarienskelette, insbesondere der Cyrtida: Zeitschrift für Wissenschaftliche Zoologie, v. 36, p. 485–540.

Bütschli, O., 1882b, Erste Band, Protozoa, *in* Bronn, H.G., ed., Klassen und Ordnungen des Thier-Reiches, Wissenschaftlich Dargestlet: Leipzig und Heidelberg: Leipzig, C.F. Winter, p. 1–482.

Campbell, A.S., 1951, New genera and subgenera of Radiolarida: Journal of Paleontology, v. 25, p. 527–530.

Campbell, A.S., 1953, A new radiolarian genus: Journal of Paleontology, v. 27, p. 296.

Campbell, A.S., 1954, Radiolaria, *in* Moore, R.C., ed., Treatise on Invertebrate Paleontology, Part. D, Protista 3: Lawrence, Kansas, Geological Society of America and University of Kansas Press, p. D11–D195.

Campbell, A.S., and Clark, B.L., 1944, Miocene radiolarian faunas from southern California: Geological Society of America, Special Papers 51, p. 1–76.

Carter, F.B., 1893, Classification of the Radiolaria: key to the species of Barbados: The American Monthly Microscopical Journal, v. 14, p. 206–213.

Carter, F.B., 1895, Classification of the Radiolaria: key to the species of Barbados: The American Monthly Microscopical Journal, v. 16, p. 81–85.

Carter, F.B., 1896a, Classification of the Radiolaria: key to the species of Barbados: The American Monthly Microscopical Journal, v. 17, p. 19–25.

Carter, F.B., 1896b, Radiolaria: a new species from Barbados: The American Monthly Microscopical Journal, v. 17, p. 25–26.

Carter, F.B., 1896c, Radiolaria: a new species from Barbados: The American Monthly Microscopical Journal, v. 17, p. 57–58.

Carter, F.B., 1896d, Radiolaria: a new genus from Barbados: The American Monthly Microscopical Journal, v. 17, p. 96–97.

Carter, F.B., 1896e, Radiolaria, a new species: The American Monthly Microscopical Journal, v. 18, p. 241–242.

Caulet, J.-P., 1991, Radiolarian from the Kerguelen Plateau, Leg 119, *in* Barron, J., Larsen, B., Baldauf, J., Alibert, C., Berkowitz, S., et al., eds., Proceedings of the Ocean Drilling Program, Scientific Results, 119: College Station, TX, USA, Ocean Drilling Program, p. 513–546.

Cavalier-Smith, T., 1999, Principles of protein and lipid targeting in secondary symbiogenesis: euglenoid, dinoflagellate, and sporozoan plastid origins and the eukaryote family tree: Journal of Eukaryotic Microbiology, v. 46, p. 347–366.

Cavalier-Smith, T., 2002, The phagotrophic origin of eukaryotes and phylogenetic classification of Protozoa: International Journal of Systematic and Evolutionary Microbiology, v. 52, p. 297–354.

Cavalier-Smith, T., 2003, Protist phylogeny and the high-level classification of Protozoa: European Journal of Protistology, v. 39, p. 338–348.

Chen, P.-H., 1975, Antarctic Radiolaria, *in* Hayes, D.E., Frakes, L.A., Barrett, P.J., Burns, D.A., Chen, P.-H., et al., eds., Initial Reports, Deep Sea Drilling Program, 28: Washington, DC, U.S. Government Printing Office, p. 437–513.

Clark, B.L., and Campbell, A.S., 1942, Eocene radiolarian faunas from the Monte Diablo area, California: Geological Society of America, Special Papers 39, p. 1–112.

Clark, B.L., and Campbell, A.S., 1945, Radiolaria from the Kreyenhagen Formation near Los Banos, California: Geological Society of America, Memoir 10, p. 1–66.

Danelian, T., Le Callonec, L., Erbacher, J., Mosher, D.C., Malone, M.J., et al., 2005, Preliminary results on Cretaceous–Tertiary tropical Atlantic pelagic sedimentation (Demerara Rise, ODP Leg 207): Comptes Rendus Geoscience, v. 337, p. 609–616.

Danelian, T., Saint Martin, S., and Blanc-Valleron, M.-M., 2007, Middle Eocene radiolarian and diatom accumulation in the equatorial Atlantic (Demerara Rise, ODP Leg 207): possible links with climatic and palaeoceanographic changes: Comptes Rendus Palevol, v. 6, p. 103–114.

De Wever, P., Dumitrică, P., Caulet, J.-P., Nigrini, C.A., and Caridroit, M., 2001, Radiolarians in the Sedimentary Record: Amsterdam, Gordon and Breach Science Publishers, 533 p.

Ehrenberg, C.G., 1839, Über die Bildung der Kreidefelsen und des Kreidemergels durch unsichtbare Organismen: Abhandlungen der Königlich Preussischen Akademie der Wissenschaften zu Berlin, Jahre 1838, p. 59–147.

Ehrenberg C.G., 1844a, Über 2 neue Lager von Gebirgsmassen aus Infusorien als Meeres-Absatz in Nord-Amerika und eine Vergleichung derselben mit den organischen Kreide-Gebilden in Europa und Afrika: Bericht über die zur Bekanntmachung geeigneten Verhandlungen der Königlich Preussischen Akademie der Wissenschaften zu Berlin, Jahre 1844, p. 57–97.

Ehrenberg, C.G., 1844b, Einige vorlaufige Resultate seiner Untersuchungen der ihm von der Sudpolreise des Captain Ross, so wie von den Herren Schayer- und Darwin zugekommenen Materialien über das Verhalten des kleinsten Lebens in den Oceanen und den grossten Bisher zuganglichen Tiefen des Weltmeeres: Monatsberichte der Königlichen Preußischen Akademie der Wissenschaften zu Berlin, Jahre 1844, p. 182–207.

Ehrenberg, C.G., 1846, Über eine halibiolithische, von Herrn R. Schomburgk entdeckte, vorherrschend aus mikroskopischen Polycystinen gebildete, Gebirgsmasse von Barbados: Bericht über die zur Bekanntmachung geeigneten Verhandlungen der Königlich Preussischen Akademie der Wissenschaften zu Berlin, Jahre 1846, p. 382–385.

Ehrenberg, C.G., 1847, Über die mikroskopischen kieselschaligen Polycystinen als mächtige Gebirgsmasse von Barbados und über das Verhältniss deraus mehr als 300 neuen Arten bestehenden ganz eigenthumlichen Formengruppe jener Felsmasse zu den jetzt lebenden Thieren und zur Kreidebildung Eine neue Anregung zur Erforschung des Erdlebens: Bericht über die zur Bekanntmachung geeigneten Verhandlungen der Königlich Preussischen Akademie der Wissenschaften zu Berlin, Jahre 1847, p. 40–60.

Ehrenberg, C.G., 1854, Mikrogeologie. Das Erden und Felsen Schaffende Wirken des Unsichtbar Kleinen Selbststandigen Lebens auf der Erde: Leipzig, Verlag von Leopold Voss, 374 p.

Ehrenberg, C.G.,1862, Übersicht die Tiefgrund-Verhältnisse des Oceans am Eingange der Davisstrasse und bei Island: Monatsberichte der Koniglichen Preussische Akademie der Wissenschaften zu Berlin, Jahre 1861, p. 275–315.

Ehrenberg, C.G., 1874, Grössere Felsproben des Polycystinen-Mergels von Barbados mit weiteren Erläuterungen: Abhandlungen der Königlich Preussischen Akademie der Wissenschaften zu Berlin, Jahre 1873, p. 213–263.

Ehrenberg, C.G., 1876, Fortsetzung der mikrogeologischen Studien als Gesammt - Uebersichtder mikroskopischen Paläontologie gleichartig analysirter Gebirgsarten der Erde, mit specieller Rücksicht auf den Polycystinen-Mergel von Barbados: Abhandlungen der Königlich Preussischen Akademie der Wissenschaften zu Berlin, Jahre 1875, p. 1–225.

Empson-Morin, K.M., 1981, Campanian Radiolaria from DSDP Site 313, Mid-Pacific Mountains: Micropaleontology, v. 27, p. 249–292.

Foreman, H.P., 1973, Radiolaria of Leg 10 with systematics and ranges for the families Amphipyndacidae, Artostrobiidae and Theoperidae, *in* Worzel, J.L., Bryant, W., Beall Jr., A.O., Capo, R., Dickinson, K., Foreman, H.P., Laury, R., McNeely, B.W., and Smith, L.A., eds., Initial Reports, Deep Sea Drilling Project, 10: Washington, DC, U.S. Government Printing Office, p. 407–474.

Frizzell, D.L., and Middour, E.S., 1951, Paleocene Radiolaria from southeastern Missouri: Bulletin of Missouri School of Mines and Metallurgy, v. 77, p. 1–41.

Funakawa, S., 1994, Plagiacanthidae (Radiolaria) from the Upper Miocene of eastern Hokkaido, Japan: Transactions and Proceedings of the Palaeontological Society of Japan, n. ser., v. 174, p. 458–483.

Funakawa, S., 1995a, Intrageneric variation and temporal change in the internal skeletal structure of plagiacanthids (Radiolaria) from Hokkaido, Japan: Transactions and Proceedings of the Palaeontological Society of Japan, n. ser., v. 180, p. 208–225.

Funakawa, S. 1995b, Lophophaeninae (Radiolaria) from the upper Oligocene to Lower Miocene and intrageneric variation in their internal skeletal structures: Journal of Geosciences, Osaka City University, v. 38, p. 13–59.

Funakawa, S., Nishi, H., Moore, T.C., and Nigrini, C.A., 2006, Data report: Late Eocene–early Oligocene radiolarians, ODP Leg 199 Holes 1218A, 1219A, and 1220A, central Pacific, *in* Wilson, P.A., Lyle, M., and Firth, J.V., eds., Proceedings of the Ocean Drilling Program, Scientific Results, 199: College Station, TX, USA, Ocean Drilling Program, p. 1–74.

Goll, R.M., 1968, Classification and phylogeny of Cenozoic Trissocyclidae (Radiolaria) in the Pacific and Caribbean basins, part I: Journal of Paleontology, v. 42, p. 1409–1432.

Haeckel, E., 1862, Die Radiolarien (Rhizopoda Radiaria). Eine Monographie: Berlin, Reimer, 572 p.

Haeckel, E., 1882, Entwurf eines Radiolarien—Systems auf Grund von Studien der Challenger—Radiolarien: Jenaische Zeitschrift für Naturwissenschaft, v. 15, p. 418–472.

Haeckel, E., 1887. Report on the Radiolaria collected by H.M.S. Challenger during the years 1873–1876: Report on the Scientific Results of the Voyage of the H.M.S. Challenger, Zoology, v. 18, 1803 p.

Hertwig, R., 1879, Der Organismus der Radiolarien: Jena, Germany, G. Fischer, 149 p.

Hollis, C.J., 2002, Biostratigraphy and paleoceanographic significance of Paleocene radiolarians from offshore eastern New Zealand: Marine Micropaleontology, v. 46, p. 265–316.

Hollis, C.J., Pascher, K.M., Sanfilippo, A., Nishimura, A., Kamikuri, S.-I., and Shepherd, C.L., 2020, An Austral radiolarian biozonation for the Paleogene: Stratigraphy, v. 17, p. 213–278.

Kling, S.A., 1971, Radiolaria, *in* Fischer, A.G., Heezen, B.C., Boyce, R.E., Bukry, D., Douglas, R.G., Garrison, R.E., Kling, S.A., Krasheninnikov, V., Lisitzin, A.P., and Pimm, A.C., eds., Initial Reports of the Deep Sea Drilling Project, 6: Washington, DC, U.S. Government Printing Office, p. 1069–1117.

https://doi.org/10.1017/jpa.2022.82 Published online by Cambridge University Press

Kozlova, G.E., 1983, Radiolarian associations of boreal regions in the lower Paleocene, *in* Lyubinova P.C., and Myatlyuk E.V., eds., The Use of Microfauna in the Study of Sediments from the Continents and Oceans (Miscellaneous Scientific Reports): Transactions of the All Union Petroleum Scientific Research Institute for Geological Survey (VNIGRI), Leningrad, p. 84–112. [in Russian]

Kozlova G.E., 1999, Paleogene boreal radiolarians from the Russia: Ministry of Natural Resources of Russian Federation, All-Russian Petroleum Research Exploration Institute (VNIGRI), Practical Manual of Microfauna, v. 9, 323 p. [in Russian]

Krasheninnikov, V.A., 1960, Some radiolarians of the Lower and Middle Eocene of the Western Pre-Caucasus, *in* Sazonov, N.T., and Shchutskaya, E.K., eds., Paleontological Collection 3: Transactions of the All Union Petroleum Scientific Research Institute for Geological Survey (VNIGRI), Leningrad, v. 16, p. 271–308. [in Russian]

Kruglikova, S.B., 1974, The characteristic species of Radiolaria in bottom sediments of the Pacific boreal zone, *in* Zhuze A.P., ed., Micropaleontology of Oceans and Seas: Academy of Sciences of the USSR, Oceanographic Commission, Moskow, p. 187–196. [in Russian]

Matsuzaki, K.M., Suzuki, N., and Nishi, H., 2015, Middle to Upper Pleistocene Polycystine radiolarians from Hole 902–C9001C, northwestern Pacific: Paleontological Research, v. 19, p. 1–77.

Meunier, M., and Danelian, T., 2022, Astronomical calibration of late middle Eocene radiolarian bioevents from ODP Site 1260 (equatorial Atlantic, Leg 207) and refinement of the global tropical radiolarian biozonation: Journal of Micropalaeontology, v. 41, p. 1–27.

Nigrini, C., 1977, Equatorial Cenozoic Artostrobiidae (Radiolaria): Micropaleontology, v. 23, p. 241–269.

Nigrini, C., Sanfilippo, A., and Moore, T.J., Jr., 2005, Cenozoic radiolarian biostratigraphy: a magnetobiostratigraphic chronology of Cenozoic sequences from ODP Sites 1218, 1219, and 1220, equatorial Pacific, *in* Wilson, P.A., Lyle, M., and Firth, J.V., eds., Proceedings of the Ocean Drilling Program: Scientific Results, v. 199, p. 1–76.

Nishimura, A., 1992, Paleocene radiolarian biostratigraphy in the northwest Atlantic at Site 384, Leg 43, of the Deep Sea Drilling Project: Micropaleontology, v. 38, p. 317–362.

O'Connor, B., 1994, Seven new radiolarian species from the Oligocene of New Zealand: Micropaleontology, v. 40, 337–350.

O'Connor, B., 1997a, Lower Miocene Radiolaria from Te Kopua Point, Kaipara Harbour, New Zealand: Micropaleontology, v. 43, p. 101–128.

O'Connor, B., 1997b, New Radiolaria from the Oligocene and early Miocene of Northland, New Zealand: Micropaleontology, v. 43, p. 63–100.

O'Connor, B., 1999a, Distribution and biostratigraphy of latest Eocene to latest Oligocene Radiolaria from the Mahurangi Limestone, Northland, New Zealand: New Zealand Journal of Geology and Geophysics, v. 42, p. 489–511.

O'Connor, B., 1999b, Distribution and biostratigraphy of latest Eocene to latest Oligocene Radiolaria from the Mahurangi Limestone, Northland, New Zealand: New Zealand Journal of Geology and Geophysics, v. 42, p. 489–511.

O'Connor, B., 2000, Stratigraphic and geographic distribution of Eocene–Miocene Radiolaria from the southwest Pacific: Micropaleontology, v. 46, p. 189–228.

O'Dogherty, L., Caulet, J.-P., Dumitrică, P., and Suzuki, N., 2021, Catalogue of Cenozoic radiolarian genera (Class Polycystinea): Geodiversitas, v. 43, p. 709–1185.

Ogane, K., Suzuki, N., Aita, Y., Sakai, T., Lazarus, D., and Tanimura, Y., 2009, Ehrenberg's radiolarian collections from Barbados, *in* Tanimura, Y., and Aita, Y., eds., Joint Haeckel and Ehrenberg Project: Reexamination of the Haeckel and Ehrenberg Microfossil Collection as a Historical and Scientific Legacy: Tokyo, Japan, National Museum of Nature and Science Monographs 40, p. 97–106.

Petrushevskaya, M.G., 1975, Cenozoic radiolarians of the Antarctic, Leg 29, DSDP, *in* Kennet, J.P., Houtz, R.E., Andrews, P.B., Edwards, A.R., Gostin, V.A., et al., eds., Initial Reports, Deep Sea Drilling Program, 28: Washington, DC, U.S. Government Printing Office, p. 541–675.

Petrushevskaya, M.G., 1984, On the classification of Polycystine radiolarians, *in* Petrushevskaya M.G., and Stepanjants, S.D., eds., Morphology, Ecology and Evolution of Radiolarians. Material from the IV Symposium of European Radiolarists EURORAD IV. Leningrad, USSR, Akademiya Nauk SSSR, Zoological Institute, p. 124–149. [in Russian]

Petrushevskaya, M.G., and Kozlova, G.E., 1972, Radiolaria: Leg 14, Deep Sea Drilling Project, *in* Hayes, D.E., Pimm, A.C., Beckmann, J.P., Benson, W.E., Berger, W.H., Roth, P.H., Supko, P.R., and von Rad, U., eds., Initial Reports, Deep Sea Drilling Program, 14: Washington, DC, U.S. Government Printing Office, p. 495–648.

Renaudie, J., Lazarus, D.B., 2012, New species of Neogene radiolarians from the Southern Ocean: Journal of Micropalaeontology, v. 31, p. 29–52.

Renaudie, J., Danelian, T., Saint-Martin, S., Le Callonec, L., and Tribovillard, N., 2010, Siliceous phytoplankton response to a Middle Eocene warming event recorded in the tropical Atlantic (Demerara Rise, ODP Site 1260A): Palaeogeography, Palaeoclimatology, Palaeoecology, v. 286, p. 121–134.

Riedel, W.R., 1957, Radiolaria: a preliminary stratigraphy, *in* Petterson, H., ed., Reports of the Swedish Deep-Sea Expedition, 1947–1948: Göteborg, Sweden, Elanders Boktryckeri Aktiebolag, v. 6, p. 59–96.

Riedel, W., 1967, Subclass Radiolaria, *in* Harland, W.B., ed., The Fossil Record: London, Geological Society of London, p. 291–298.

Riedel W.R., and Campbell, A.S., 1952, A new Eocene radiolarian genus: Journal of Paleontology, v. 26, p. 667–669.

Riedel, W.R., and Sanfilippo, A., 1970, Radiolaria, Leg 4, Deep Sea Drilling Project, *in* Bader, R.G., Gerard, R.D., Benson, W.E., Bolli, H.M., Hay, W.W., Rothwell, Jr., T., Ruef, M.H., Riedel, W.R., and Sayles, F.L., eds., Initial Reports, Deep Sea Drilling Program, 4: Washington, DC, U.S. Government Printing Office, p. 503–575.

Riedel, W.R., and Sanfilippo, A., 1971, Cenozoic Radiolaria from the western equatorial Pacific, Leg 7, *in* Winterer, E.L., Riedel, W.R., Brönnimann, P., Gealy, E.L., Heath, G.R., Kroenke, L., Martini, E., Moberly Jr., R., Resig, J., and Worsley, T., eds., Initial Reports, Deep Sea Drilling Program, 28: Washington, DC, U.S. Government Printing Office, p. 1529–1672.

Riedel, W.R., and Sanfilippo, A., 1978, Stratigraphy and evolution of equatorial Cenozoic radiolarians: Micropaleontology, v. 24, p. 61–96.

Sandin, M.M., Pillet, L., Biard, T., Poirier, C., Bigeard, E., Romac, S., Suzuki, N., and Not, F., 2019, Time calibrated morpho-molecular classification of Nassellaria (Radiolaria): Protist, v. 170, p. 187–208.

Sanfilippo, A., and Caulet, J.-P., 1998, Taxonomy and evolution of Paleogene Antarctic and tropical Lophocyrtid radiolarians: Micropaleontology, v. 44, p. 1–43.

Sanfilippo, A., and Riedel, W.R., 1970, Post-Eocene "closed" theoperid radiolarians: Micropaleontology, v. 16, p. 446–462.

Sanfilippo, A., and Riedel, W.R., 1973, Cenozoic Radiolaria (exclusive of theoperids, artostrobiids and amphipyndacids) from the Gulf of Mexico, DSDP Leg 10, *in* Worzel, J.L., Bryant, W., Beall Jr., A.O., Capo, R., Dickinson, K., Foreman, H.P., Laury, R., McNeely, B.W., and Smith, L.A., eds., Initial Reports, Deep Sea Drilling Program, 10: Washington, DC, U.S. Government Printing Office, p. 475–611.

Sanfilippo, A., and Riedel, W.R., 1982, Revision of the radiolarian genera *Theocotyle*, *Theocotylissa* and *Thyrsocyrtis*: Micropaleontology, v. 28, p. 170–188.

Sanfilippo, A., and Riedel, W.R., 1992, The origin and evolution of Pterocorythidae (Radiolaria); a Cenozoic phylogenetic study: Micropaleontology, v. 38, p. 1–36.

Sanfilippo, A., Westberg-Smith, M.J., and Riedel, W.R., 1985, Cenozoic Radiolaria, *in* Bolli, H.M., Saunders, J.B., and Perch-Nielsen, K., eds., Plankton Stratigraphy: Cambridge, UK, Cambridge University Press, p. 631–712.

Saunders, J.B., Bernoulli, D., Mueller-Merz, E., Oberhaensli, H., Perch-Nielsen, K., Riedel, W.R., Sanfilippo, A., and Torrini, R., Jr., 1984, Stratigraphy of the late middle Eocene to early Oligocene in the Bath Cliff section, Barbados, West Indies: Micropaleontology, v. 30, p. 390–425.

Schneider, C.A., Rasband, W.S., and Eliceiri, K.W., 2012, NIH Image to ImageJ: 25 years of image analysis: Nature Methods, v. 9, p. 671–675.

Shipboard Scientific Party, 2004, Site 1260, *in* Erbacher, J., Mosher, D.C., Malone, M.J, Berti, D., Bice, K.L., et al., eds., Proceedings of the Ocean Drilling Program: Initial Reports, v. 207, p. 1–113.

Strelkov, A.A., and Lipman, R.K., 1959, Podclass Radiolaria. Sistematicheskaya chast, *in* Khabakov, A.V., ed., Osnovy Paleontologii, vol. 1. Radiolyarii: Izdatelstvo Akademiya Nauk SSSR, Moscow, USSR, p. 369–482. [in Russian]

Suganuma, Y., and Ogg, J.G., 2006, Campanian through Eocene magnetostratigraphy of sites 1257–1261, ODP leg 207, Demerara rise (Western Equatorial Atlantic), *in* Mosher, D.C., Erbacher, J., Malone, M.J., Berti, D., Bice, K.L., et al., eds., Proceedings of the Ocean Drilling Program: Scientific Results, v. 207, p. 1–48.

Sugiyama, K., 1998, Nassellarian fauna from the Middle Miocene Oidawara Formation, Mizunami Group, central Japan: News of Osaka Micropaleontologists, Special Volume 11, p. 227–250. [in Japanese]

Sutton, H.J., 1896a, Radiolaria; a new species from Barbados: The American Monthly Microscopical Journal, v. 17, p. 58–60.

Sutton, H.J., 1896b, Radiolaria; a new genus from Barbados: The American Monthly Microscopical Journal, v. 17, p. 61–62.

Sutton, H.J., 1896c, Radiolaria; a new genus from Barbados: The American Monthly Microscopical Journal, v. 17, p. 138–139.

Sutton, H.J., 1896d, Radiolaria; two new species from Barbados: The American Monthly Microscopical Journal, v. 17, p. 161–163.

Suzuki, N., O'Dogherty, L., Caulet, J.-P., and Dumitrică, P., 2021, A new integrated morpho- and molecular systematic classification of Cenozoic radiolarians (Class Polycystinea)—suprageneric taxonomy and logical nomenclatorial acts: Geodiversitas, v. 43, p. 405–573.

Takemura, A., and Ling, H.Y., 1998, Taxonomy and phylogeny of the genus *Theocorys* (Nassellaria, Radiolaria) from the Eocene and Oligocene sequences in the Antarctic region: Paleontological Research, v. 2, p. 155–169.

https://doi.org/10.1017/jpa.2022.82 Published online by Cambridge University Press

Wang, X., Reinhard, C.T., Planavsky, N.J., Owens, J.D., Lyons, T.W., and Johnson, T.M., 2016, Sedimentary chromium isotopic compositions across the Cretaceous OAE2 at Demerara Rise Site 1258: Chemical Geology, v. 429, p. 85–92.

Westerhold, T., and Röhl, U., 2013, Orbital pacing of Eocene climate during the middle Eocene climate optimum and the chron C19r event: missing link found in the tropical western Atlantic: Geochemistry, Geophysics, Geosystems, v. 14, p. 4811–4825.

Witkowski, J., Bohaty, S.M., McCartney, K., and Harwood, D.M., 2012, Enhanced siliceous plankton productivity in response to middle Eocene warming at Southern Ocean ODP Sites 748 and 749: Palaeogeography, Palaeoclimatology, Palaeoecology, v. 326–328, p. 78–94.

Accepted: 1 September 2022

https://doi.org/10.1017/jpa.2022.82 Published online by Cambridge University Press